

AD-A208 181

1

31 December 1988
POLY-WRI-1554-89

ANNUAL REPORT
on
BASIC RESEARCH IN
ELECTRONICS (JSEP)

CONTRACT NO. F49620-88-C-0075
1 APRIL 1988 TO 31 DECEMBER 1988

Erich E. Kunhardt
JSEP Principal Investigator
and Program Director

POLYTECHNIC UNIVERSITY
WEBER RESEARCH INSTITUTE
FARMINGDALE, NY 11735

DTIC
ELECTE
MAY 26 1989
S D
cb D

DISTRIBUTION STATEMENT A
Approved for public release;
Distribution Unlimited

008

REPORT DOCUMENTATION PAGE

1a. REPORT SECURITY CLASSIFICATION		1b. RESTRICTIVE MARKINGS	
2a. SECURITY CLASSIFICATION AUTHORITY UNCLASSIFIED		3. DISTRIBUTION / AVAILABILITY OF REPORT Approved for public release; distribution unlimited.	
2b. DECLASSIFICATION / DOWNGRADING SCHEDULE			
4. PERFORMING ORGANIZATION REPORT NUMBER(S) POLY-WRI-1554-89		5. MONITORING ORGANIZATION REPORT NUMBER(S)	
6a. NAME OF PERFORMING ORGANIZATION Weber Research Institute Polytechnic University	6b. OFFICE SYMBOL (If applicable)	7a. NAME OF MONITORING ORGANIZATION Air Force Office of Scientific Research/NE	
6c. ADDRESS (City, State, and ZIP Code) Route 110 Farmingdale, NY 11735		7b. ADDRESS (City, State, and ZIP Code) Bolling Air Force Base Washington, DC 20332	
8a. NAME OF FUNDING / SPONSORING ORGANIZATION Air Force Office of Scientific Research/NE	8b. OFFICE SYMBOL (If applicable) NE	9. PROCUREMENT INSTRUMENT IDENTIFICATION NUMBER F49620-88-C-0075	
8c. ADDRESS (City, State, and ZIP Code) Bolling Air Force Base Washington, D.C. 20332		10. SOURCE OF FUNDING NUMBERS	
		PROGRAM ELEMENT NO.	PROJECT NO.
11. TITLE (Include Security Classification) Basic Research in Electronics (JSEP) (Unclassified)			
12. PERSONAL AUTHOR(S) Erich E. Kunhardt			
13a. TYPE OF REPORT Annual Report	13b. TIME COVERED FROM 1-4-88 TO 12-31-88	14. DATE OF REPORT (Year, Month, Day) 88 December 31	15. PAGE COUNT 57
16. SUPPLEMENTARY NOTATION			
17. COSATI CODES		18. SUBJECT TERMS (Continue on reverse if necessary and identify by block number) Electromagnetics, microwaves, millimeter waves, waveguides and antennas, optics, x-rays, solid state interactions and materials, information electronics, image restoration.	
FIELD	GROUP		
19. ABSTRACT (Continue on reverse if necessary and identify by block number) This report presents a summary of the scientific progress and accomplishments on research projects in the Joint Services Electronics Program (JSEP) for the contract period from 1 April 1988 through 31 December 1988. It also includes work accomplished under Contract No. F49620-85-C-0078 from 1 January 1988 to 31 March 1988. The Joint Services Electronics Program at Polytechnic University is the core of interdisciplinary research in electronics encompassing programs in the Department of Electrical Engineering, Physics, and Chemistry under the aegis of the Weber Research Institute. The research encompassed by this program is grouped under two broad categories: Interactions of Wide-Band Electromagnetic Radiation with Complex Macro- and Micro-Structures (EM) and Field-Particle Interactions in Matter: Single Particle, Collective and Cooperative Phenomena (FP). The detailed projects (research units) comprising the complete program are listed in the Table of Contents. (2471)			
20. DISTRIBUTION / AVAILABILITY OF ABSTRACT <input type="checkbox"/> UNCLASSIFIED/UNLIMITED <input type="checkbox"/> SAME AS RPT. <input type="checkbox"/> DTIC USERS		21. ABSTRACT SECURITY CLASSIFICATION UNCLASSIFIED	
22a. NAME OF RESPONSIBLE INDIVIDUAL Erich E. Kunhardt, Director		22b. TELEPHONE (Include Area Code) (516) 755-4250	22c. OFFICE SYMBOL

TABLE OF CONTENTS

Section	Page
DD Form 1473	
DIRECTOR'S OVERVIEW	i
SIGNIFICANT SCIENTIFIC ACCOMPLISHMENTS	ii
SECTION I. INTERACTIONS OF WIDE-BAND ELECTROMAGNETIC RADIATION WITH COMPLEX MACRO- AND MICRO-STRUCTURES (EM)	
A. Wide-Band Electromagnetic Wave Interaction With Large Aperture-Coupled Enclosures	1
B. Microparticle Photonics	25
C. Beam-Field Interactions in Nonlinear Thin Films	31
SECTION II. FIELD-PARTICLE INTERACTIONS IN MATTER	
A. Resonant Interactions in Crystals at X-ray Wavelengths	41
B. Resonances in X-ray Phonon Interactions in Crystals	51
C. Non-Equilibrium Wave Cooper Pair Interaction in High T_c Superconductors	55



Accession For	
NTIS CRA&I	<input checked="" type="checkbox"/>
DTIC TAB	<input type="checkbox"/>
Unannounced	<input type="checkbox"/>
Justification	
By _____	
Distribution/	
Availability Codes	
Dist	Avail and/or Special
A-1	

DIRECTOR'S OVERVIEW

This report presents a summary of the scientific progress and accomplishments on research projects funded by the Joint Services Electronics Program (JSEP) for the contract period from 1 April 1988 through 31 December 1988. It also includes work accomplished under CONTRACT NO. F49620-85-C-0078 from 1 January 1988 to 31 March 1988. It does not contain information regarding accomplishments on research projects funded in other ways.

The Joint Services Electronics Program at Polytechnic University is the core of interdisciplinary research in electronics conducted by faculty members of the in the Departments of Electrical Engineering, Physics and Chemistry under the aegis of the Weber Research Institute. The Weber Research Institute JSEP Director and Principal Investigator is Professor Erich Kunhardt. He is responsible for the selection of the best individual proposals, coordination between Polytechnic University and the JSEP TCC and coordination between the selected areas of the JSEP Program. In planning the JSEP Program at WRI, a general objective is to develop new projects with 3-6 years of JSEP sponsorship, leading to transition to DoD or other agency program funding. This report covers the first year of our current 3 year cycle. The research encompassed by this program is grouped into two broad categories: Interactions of Wide-Band Electromagnetic Radiation with Complex Macro- and Micro-Structures (EM) and Field-Particle Interactions in Matter: Single Particle, Collective and Cooperative Phenomena (FP). The detailed projects (research units) comprising the complete program are listed in the Table of Contents.

Following our previous practice, Section 2 of every research unit contains a short *summary* of the recent progress. Further details regarding that progress are contained in Section 3, State of the Art and Progress Details.

Each of the research units described in this report is designated, for example, as EM8-1 or FP8-1, corresponding the the category, year (1988) and the number within the category. These numbers follow the numbers given in our proposal dated 1 July 1987 except that each proposed unit which was phased out in accord with instructions of the TCC has been eliminated and the number of each subsequent project was reduced by one.

Folowing this Overview, we present a *Report on Significant Scientific Accomplishments* which highlights important contribution this year.

REPORT ON SIGNIFICANT ACCOMPLISHMENTS

December 31, 1988

High Frequency Propagation at Long Ranges near a Concave Boundary (T. Ishihara* and L.B. Felsen)

High frequency propagation along and near a concave boundary excited by a source close to the boundary exhibits anomalous effects attributable to the failure of ray theory for the high-order multiply reflected fields. For moderate values of the universal parameter $\gamma = (ka/2)^{1/3}s/a$, where k is the wavenumber, "a" is the boundary radius and s is the propagation distance along the boundary, the anomalies can be accounted for by a self-consistent combination of legitimate ray fields (with moderate number of reflections) and a few whispering gallery modes. This parametrization becomes deficient for very large γ , corresponding to long propagation distances and (or) very weak surface curvature. A new hybrid ray-parabolic equation (PE) scheme has been developed that replaces the whispering gallery modes by a beam-type propagator. This scheme, which is efficiently implemented numerically, accommodates the large γ domain not only for the prototype circular boundary that serves to generate an independent reference solution, but also for variable radius of curvature, including concave-to-convex transitions. The earlier ray-mode parametrization fails completely for concave-convex surface contours.

(1) * Department of Electrical Engineering, National Defense Academy, Hashirimizu, Yokosuka 239, Japan.

**SECTION I:
INTERACTIONS OF WIDE-BAND ELECTROMAGNETIC
RADIATION WITH COMPLEX MACRO- AND MICRO-STRUCTURES (EM)**

A. WIDE-BAND ELECTROMAGNETIC WAVE INTERACTION WITH LARGE APERTURE-COUPLED ENCLOSURES

Profs. L.B. Felsen and I-T. Lu

Unit EM8-1

1. OBJECTIVE(S)

Present technologies relating to communication, surveillance, identification, and other similar tasks demand understanding of the interaction of electromagnetic waves with complex penetrable environments, with the need becoming increasingly more acute for future system development, and with a trend toward wide-band operation in successively higher ranges of frequencies. The environments can be natural (like the earth and its substructure, the troposphere, or the ionosphere) or man-made (like integrated-electronics circuits, aircraft, vehicles or buildings). The objective of this long term research program is to *parameterize* the electromagnetic field in complex environments in terms of "good observables" that can be coordinated with the form of the detected signal. Such a parametrization can then be employed to *predict* the interior-exterior response, to *classify* the environment, and to lay the basis for the *inverse* problem of identification. To achieve this goal, *new analytical techniques* must be developed for coping with *electrically large partially enclosed complex* configurations which have *no* apparent *symmetries*. The problem will be attacked by classifying structural interior and exterior units on the scale of the wavelengths contained in the spectrum of the electromagnetic signal, and exploring the self-consistent dynamic interaction of these units to produce the overall response. *New wave phenomena* - both fundamental (canonical) and interactive, and based on physical phenomenology - will be sought for providing "good" building blocks in the parametrization scheme.

2. SUMMARY OF RECENT PROGRESS

This section presents a brief summary of recent progress; a more detailed description is contained in section 5.

Three problems are being investigated. The first test is to construct the complex resonances of an open-ended plane parallel waveguide cavity. A global resonance formulation including all ray field interactions between reflection and diffraction centers has been derived. These interactions have been grouped so as to distinguish between interior and exterior effects. We also formulate partial resonances which highlight the interior and exterior effects separately by decoupling the external from the internal. Modal reflection and coupling coefficients have been constructed and numerical implementation of the radar cross section algorithm has been initiated.

The second study involves a new method which combines the hybrid ray-mode and boundary element methods. The latter is used to formulate the aperture scattering process and the former to provide the Green's function of the layered environment. Numerical implementations have been initiated for computing both source-excited and source-free problems for a test configuration involving a perfectly conducting, thin-walled plane parallel waveguide whose interior is coupled to the exterior by an aperture in one of the walls.

The third study embodies a substantial generalization of that for the first test problem. A slit-coupled complex perfectly conducting thin cylindrical shell with interior convex perfectly conducting cylindrical loading is being investigated via the external-ray and internal-local mode formulation. The prediction of the location of the resonance spikes in the bistatic scattering cross section is pursued by a perturbation scheme.

3. STATE OF THE ART

The state of the art in this problem area has been a *piecemeal approach* wherein disconnected strategies have been brought to bear on different parametric regimes. For wavelengths that are larger or at most comparable with the scale of the entire structure, boundary integral equation [1] and T-matrix techniques [2] can attack moderately complex structural shapes, while numerical methods involving finite element and finite difference schemes [3] can model more substantial complexity. The required computational effort is appreciable, and the result, even when numerically reliable, provides no explanation of the wave phenomena that are operative in producing the response.

For shorter wavelengths, the problems become successively "larger" in a computational sense, and overall direct numerical modeling by the above-mentioned and other similar approaches is no longer feasible. One may now attempt to extract global information about the structure by determining its "resonances", which are field patterns (eigenstates) that maintain themselves at their characteristic resonant frequencies without external excitation. The resonances are undamped for lossless fully enclosed systems (closed cavities) but damped (with complex resonant frequencies) when the structure has access to, or is embedded within, an infinite space. The resonances are broad, and decay rapidly, for low-Q structures (either due to loss or due to strong radiation damping), but can be narrow and highly peaked for high-Q aperture coupled interiors. The most significant and reliably resolvable resonances are those at the lower frequency end where overall dimensions are not substantially larger than the signal wavelength. Thus, the corresponding data processing schemes eliminate the high frequency portion of the signal spectrum. Within the context of transient signal scattering, the resonance approach is known as the singularity expansion method (SEM) because the complex resonances appear as pole singularities in the complex frequency plane; observations (pro and con)

pertaining to its implementation for *exterior* problems may be found in the recent literature [4-9]. Basically, the algorithm requires a good signal to noise ratio, and its ability to resolve structural detail is limited by the inherent *global* nature of the resonances and the concentration on the lower frequency end.

When the wavelengths are small compared not only to the overall extent of the structure but also to structural features (substructures) within the conglomerate, the ray techniques of the geometrical theory of diffraction (GTD), asymptotic techniques associated with physical optics (PO), and related procedures become applicable [10]. These procedures can also be employed for transient analysis near the wavefronts of the impinging signal. However, their implementation so far has been primarily for *exterior* scattering.

The proposed program is *new* because it addresses a class of complex electromagnetic wave interaction problems that has not been explored heretofore. Its implementation requires a thorough understanding of waves and spectra, of asymptotic techniques for localization, of the interrelation between rays, modes, wavefronts, resonances, and other similar "good observable", etc. The groundwork for the new extensions has been laid in our previous pioneering studies of wave phenomena under the JSEP program. Results from these studies have been reported in a large number of publications, a sample of which is included in [11-25].

4. PROPOSED RESEARCH PROGRAM

A. Problem Strategy

The solution strategies described in Section 3 are tailored to distinct portions of the signal spectrum, without mutual connection. Moreover, in the short wavelength range, they address almost exclusively the *exterior* problem. In the new scenario proposed here, the wide-band scattering problem will be treated in its entirety. By the scale of the wavelengths in various portions of the signal spectrum, it will be attempted to decide whether the behavior of the electromagnetic field in constituent parts of a complex system is determined primarily by guiding, leakage, diffraction, resonance, or disarray that is best described stochastically. The overall system will then be analyzed by self-consistent interaction among these constituent parts. To effect this characterization, it is necessary to study the time-harmonic behavior over a range of frequencies, and also the impulse-excited behavior when appropriate. The resulting information forms the basis for self-consistent synthesis of the response to transient excitation.

The analytical machinery for implementation of this adaptive approach will be structured around new concepts in the treatment of wave spectra, both in the space (wavenumber) and time (frequency) domains. As mentioned in Section 3, the background for the concepts can be found in our previous work; the spectral building

blocks in the frequency or time domain involve real and complex rays and modes, or wavefronts and resonances, as well as their self-consistent hybrid combinations. These concepts need to be generalized and tested under new conditions, and entirely new methodologies will be sought out, in addition. One of these is the method of "shooting" rays (Fig. 1), through which one establishes in the high frequency region those domains within a complex structure where high field intensities are produced; in its simplest version, this method has been used in seismology [26,27], but it is new to electromagnetics and will be refined for these applications. Another, which is particularly exciting in this spectral game, involves new rigorous representations of general (actual or induced) source distributions in terms of basis functions (for example, Gaussians) in a *discretized* (time-frequency) and (space-wavenumber) phase space [28,29].

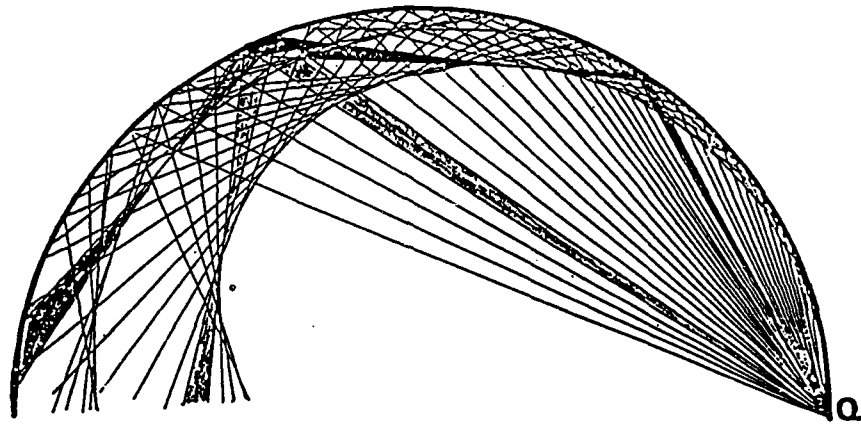


Fig. 1

Ray shooting due to edge diffraction on a concave boundary. Ray traces depict multiple reflection, and formation of caustics, where closely adjacent rays intersect. The caustics indicate regions of enhanced field strength but ray theory fails near the caustics. Ray shooting algorithms are readily implemented on a computer. Beam shooting algorithms are also readily implemented for *paraxial beams*, and they are *finite* at caustics. But paraxial beam algorithms have unpredictable accuracy. We shall explore schemes for correcting the deficiencies of these algorithms.

Because Gaussian basis fields have favorable propagation properties, this places new relevance on our previous studies of time-harmonic and transient Gaussian beams (especially our complex source point method), and on their interaction with various environments [23,30-35]. Gaussian beam fields are not only natural descriptors of energy concentration by focusing, they also serve to smooth out radical changes in

behavior associated with transitions from one wave process to another, and therefore are favored in numerical algorithms.

The testing of the proposed ideas will be performed on canonical problems, initially in coordinate-separable geometries which permit analysis by rigorous methods. The essential ingredient here is to cast the solution into a form that highlights the various postulated wave processes as enumerated above, with numerical comparisons to establish when these processes are optimally excited and therefore furnish "good" characterizations. Furthermore, these good characterizations will be phrased so that they can be *generalized* when the configuration departs from the canonical model, i.e., they must be *phenomenologically robust* under gradual changes in the environment. By this strategy, which requires an intricate interplay of global and local wave phenomena, it is envisioned to provide eventually a catalog of interactions, by which complex systems can be analyzed as interacting subsystems [8], with the latter chosen by their predominant response characteristics under the given conditions of excitation.

B. Test Geometries

Canonical test geometries have been selected for consideration. The first, already well advanced, is the classical open-ended parallel plane waveguide, but the solution strategy has been cast in a *new* format that clarifies the hybrid ray-beam-mode interplay for plane wave coupling into, and radiation out of, this configuration at *very small wavelength-to-plate spacing ratios* [24]. The more complicated semi-infinite circular waveguide has also been considered from this new perspective [25].

Next will be the non-classical configurations of wave coupling into, and out of, a thin slitted circular cylinder, first empty inside, and then with interior and(or) exterior loading (see Fig. 2). From parametric studies for various slit width-to-diameter ratios, and for various ranges of wavelengths, we shall seek to ascertain robust characterizations in terms of self-consistent combinations of direct and edge-diffracted ray fields on the inside and outside, whispering galley modes on the concave interior portion, etc. The ray shooting method will also be tried out here. Furthermore, the construction of full and partial complex resonances by cumulative treatment of multiple interactions, and the corresponding partition of the overall structure into interacting substructures, will be considered, as will the influence of these scenarios on the characterization of the interior field and the target signature. For reference, we shall make use of available reliable numerical solutions [36]. We also plan to obtain experimental verification at optical frequencies by utilizing the laser technology resident within the Group on Wave Particle Interactions. Efforts will be made to design these experiments so that they can actually implement the ray shooting algorithm.

Another prototype structure, in spherical-conical coordinates (Fig. 3), is intended to model effects of large complicated cavity-like enclosures with *non-parallel, non-*



Fig. 2 Slitted cylinder cavity
(a) without loading
(b) with loading.

planar walls. Depending on the choice of the boundary surfaces, this configuration can model a shell-like enclosure of broad lateral extent (Fig. 3a), an elongated enclosure with curved (Fig. 3b) or straight (Fig. 3c) axis and a broad variety of other structural features. External coupling can be provided through any single boundary surface (when completely removed), or through apertures in any of these surfaces. Emphasis here shall be especially on the tracking of local modes, which are defined by periodicities (local eigenvalues) appropriate to the local spacing between the boundaries along one of the coordinates, and which follow *ray* trajectories in the lateral domain defined by the remaining two coordinates (Fig. 3a) [37,38]. This prototype study will clarify the validity of the (local mode)-(lateral ray) concept under quite general conditions.

5. PROGRESS DETAILS

The long term research program described above charts a *systematic* course toward gaining an understanding of the electromagnetic wave response of large complex interior-exterior environments under wide band signal illumination. Results from these studies will provide a catalog of "good observables," which parameterize a complex system in terms of *physical meaningful* interacting subsystems. Such a parametrization will have direct impact on prediction of overall performance, on ascertaining field penetration into the interior, on signature interpretation, and eventually on identification, of complex configurations.

Currently we are investigating three problems to test and demonstrate the utility of these techniques.

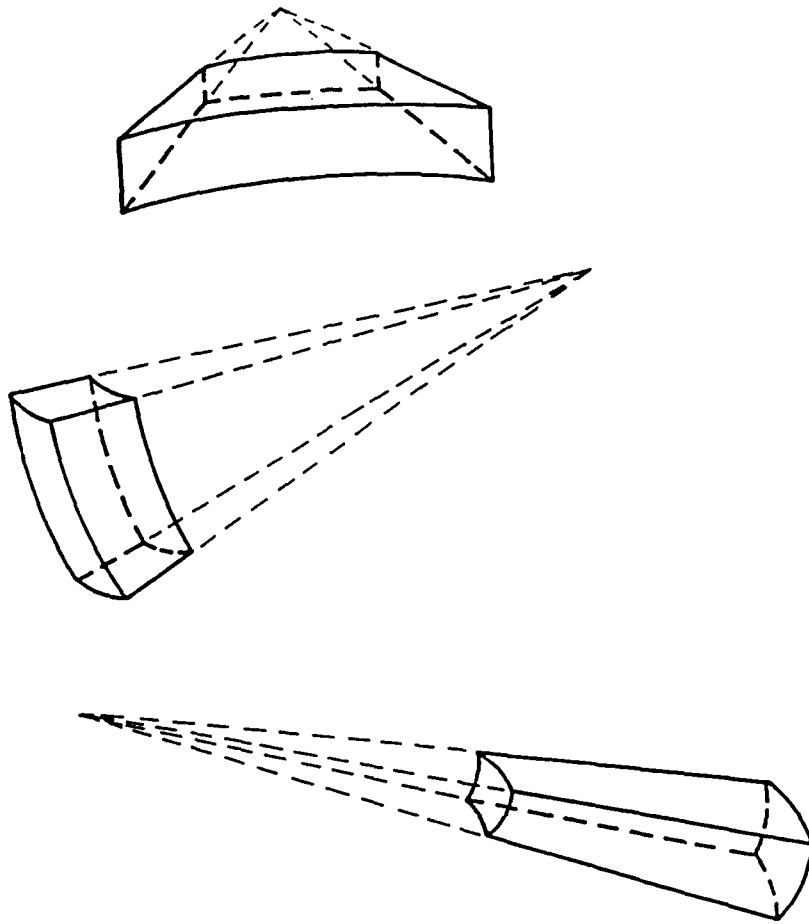


Fig. 3 Prototype structures, in spherical-conical coordinates, to model large complicated cavity-like enclosures.

A. Complex Resources of an Open Ended Plane Parallel Waveguide Cavity*

1. General Remarks

For a first test of the problem strategy outlined in Sec. 4, we have chosen as a cavity geometry a thin-walled, perfectly conducting, infinitely long rectangular trough shown in Fig. 4. This prototype structure has the following desirable attributes:

(*) This phase is being worked on by E. Heyman, G. Friedlander and L.B. Felsen.

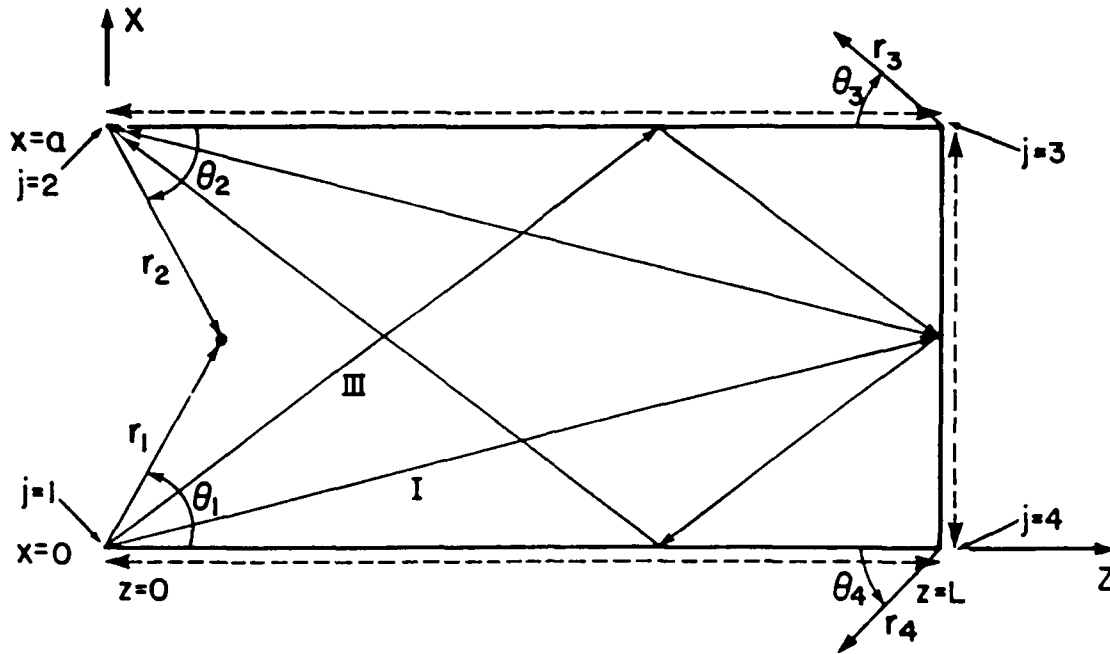


Fig. 4 Thin-walled rectangular trough of infinite length along y . Relevant internal and external ray interactions are schematized by solid and dashed lines, respectively, with the interior Roman numerals identifying the number of (internal) reflections between diffraction events at the edges $j=1,2$. The sketch includes up to three internal reflections. Local coordinates (r_j, θ_j) identify phenomena associated with edge j .

- (a) It models interior-external effects.
- (b) Being comprised of plane surfaces terminated in straight edges or corners, it permits description of the propagation, reflection diffraction and interaction mechanisms experienced by an incoming signal in a simple manner, without obscuring the physics of the process by mathematical complexities.
- (c) Since the spacing between the sides is considerably less than their length, the interior portion can be viewed as plane parallel waveguide which is open at one end and closed at the other; this is a simple environment for introduction of guided modes as alternatives to multiple reflected wavefronts.
- (d) The various constituent portions (edges, corners, open waveguide end) constitute classical and rigorously solvable diffraction problems with known solutions [25], thereby facilitating assessment of the quality of asymptotic and other approximations when implementing the wavefront, partial resonance, and hybrid wavefront-resonance schemes. Thus, the test configuration is ideal for exploring wavefront or ray fields (which are non-dispersive); guided modes (which are dispersive); high-Q phenomena due to partial internal resonances; low-Q

phenomena due to external effects which are expressed much more suitably by ray interactions than by partial external resonances; and the interaction of all of these constituent wave processes in a well parametrized format.

To proceed, we first cast the previously developed general wavefront-resonance-partial resonance procedure [8] in a form that associates the partial internal resonances explicitly with the guided modes. This is expected to lead to a good parametrization of the global scattering behavior provided that the signal spectrum has an upper cutoff which keeps the number of propagating waveguide modes within acceptable limits. The derivation shows how the internal wavefront interactions are treated collectively via the guided modes (propagating and evanescent), and that the eigenvectors of the matrix resonance equation play a direct role in describing self-consistently the mode coupling due to an open end. It is also shown how the more prominent internal resonances are loaded by the much weaker external effects which are adequately retained as ray interactions. The format thus being set, we address the quantitative description of internal and external wavefront (ray) interactions (like those in the interior) in partial resonance form. Various partial resonance options are played out, the most important being those that neglect intermode coupling entirely or account for it selectively. Numerical implementation is presently in progress. Preliminary results for interior partial resonances are shown in Fig. 5.

2. Formulation of the Scattering Problem

i. Global resonance formulation

In the frequency domain, with suppressed dependence $\exp(-i\omega t)$, the self-consistent formulation of the scattering problem by multiple ray interactions may be found in Eqs. (8a) and (8b) of reference [8]. The ray field interaction between scattering centers, denoted by indices i and j , is given in Eq. (4) of reference [8], and it encompasses the high frequency asymptotic approximation of the geometrical theory of diffraction (GTD) [10]. With an evident change of notation, it is written here as follows

$$S_{ij}(\omega) \sim A_{ij}(\omega)\exp(ikL_{ij}), \quad k = \omega/v \quad (1)$$

where ω is the radian frequency, A_{ij} is the excitation (diffraction) coefficient at j , and L_{ij} is the propagation path (ray trajectory) from i to j . The ray interaction functions S_{ij} can be organized as elements in a ray interaction matrix S .

Because of the *multiple* undamped internal ray reflections in the present application, it is desirable to re-express some or all of these internal interactions collectively in terms of the guided modes. The restructuring is done most generally in a hybrid ray-mode representation whereby various angular spectrum intervals centered at the edges $j=1,2$ can be filled either with rays or modes, depending on which species has the most favorable properties there. Details of this procedure are given in [24]. This most versatile approach is not pursued here; instead, *all* of the internal ray fields are replaced by the complete set of modes propagating (or

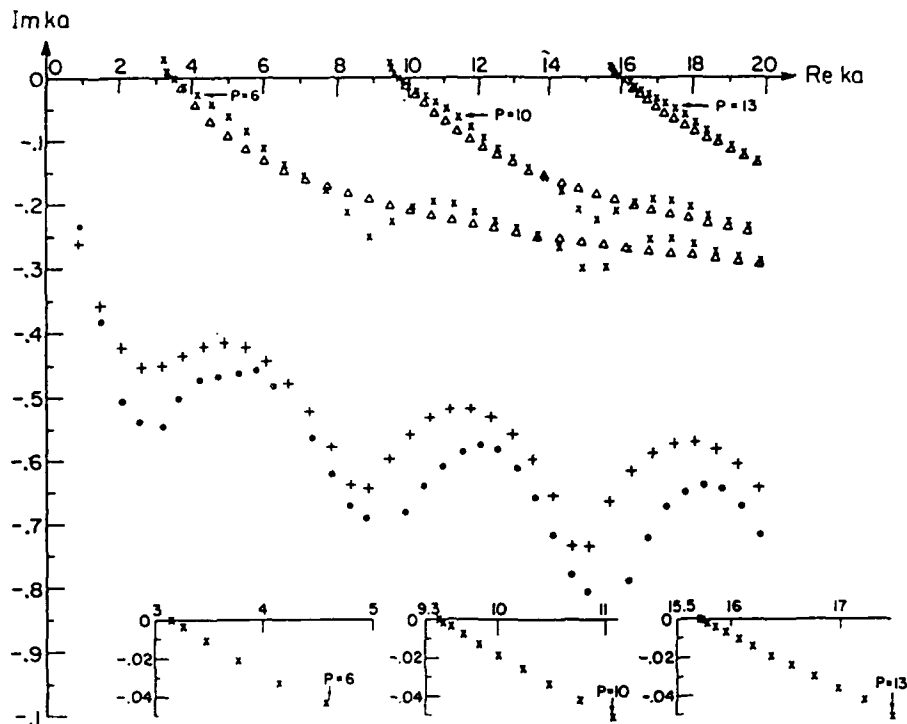


Fig. 5

Partial resonances corresponding to antisymmetric fields. Internal TM_n resonances (n odd) without mode coupling and with the following $\bar{\Gamma}_{n,n}$ models computed from (16) and (19): $\Delta\Delta\Delta$ - single edge diffraction without external coupling; the near-cutoff resonances lie too close to the triple diffraction values to be plotted on the graph; xxx - triple edge diffraction without external coupling; $+++$ - external resonances (antisymmetric) without internal coupling; \dots - TM_1 mode resonances (triple diffraction) coupled to external interactions by including the effects in (22). The influence of the coupling on the external resonances is as shown (\cdot); the effect on the internal resonances is too small to be distinguished from the xxx on the graph.

The asymptotic results from (16) and (19) are inaccurate near mode cutoffs. The correct results obtained from (16), with (21), are shown in the insets. The resonances in the insets can be related to those in the main resonance map by using the arrows that identify resonances with the same index p for which the two representations give almost identical results.

evanescent) along the z direction of Fig. 4. Interaction centers for these modes are at the open end $z=0$ and the closed end $z=L$. With n denoting the mode index, a typical mode field has the form

$$u_n^\pm(x,z) = V_n^\pm \exp(\pm i\kappa_n z) \psi_n(x) \quad (2)$$

where $\kappa_n = (k^2 - k_{x_n}^2)^{1/2}$ is the modal propagation coefficient, $\psi_n(x)$ describes the transverse mode shape, and V_n represents the modal amplitude. The paired plus and

minus signs go with propagation along the (+z) and (-z) directions, respectively. For the perfectly conducting plane parallel waveguide with width a , the transverse eigenvalues are $k_{x_n} = n\pi/a$, and the mode shapes are

$$\cos k_{x_n} x, \quad n = 0, 1, 2, \dots, \quad \text{for TM polarization} \quad (3a)$$

$$\psi_n(x) = \begin{cases} \cos k_{x_n} x, & n = 0, 1, 2, \dots, \quad \text{for TM polarization} \\ \sin k_{x_n} x, & n = 1, 2, \dots, \quad \text{for TE polarization} \end{cases} \quad (3b)$$

The modal amplitudes V_n^+ and V_n^- can be assembled as elements in column vectors \underline{V}^+ and \underline{V}^- , respectively. If their phase reference is placed at $z=0$, the perfect reflection condition at $z=L$ leads to the following relation between \underline{V}^- and \underline{V}^+ ,

$$\underline{V}^- = \bar{\Gamma} \underline{V}^+, \quad \bar{\Gamma} = \text{diag} [\bar{\Gamma}_{nn}], \quad (4)$$

where $\bar{\Gamma}$ is a diagonal matrix whose elements account for the round trip phase accumulation

$$\bar{\Gamma}_{nn} = \pm \exp(i2\kappa_n L) \quad (4a)$$

and the upper and lower signs apply to the TM or TE polarization, respectively. Similarly, looking from $z=0^+$ toward the open end at $z=0$, one has the relation

$$\underline{V}^+ = \bar{\Gamma} \underline{V}^-, \quad \bar{\Gamma} = [\bar{\Gamma}_{mn}] \quad (5)$$

where $\bar{\Gamma}_{mn}$, $m \neq n$, expresses the intermodal coupling, and $\bar{\Gamma}_{nn}$ the modal reflection coefficient. These coefficients account for *total* effects at the edges $j=1,2$ in Fig. 4, and include modal excitations from the inside as well as external ray field returns due to all interactions involving edges $j=3,4$. Combining (4) and (5) leads to the self-consistency condition

$$\underline{R} \underline{V}^+ = 0, \quad \underline{R} = \underline{I} - \bar{\Gamma} \bar{\Gamma} \quad (6a)$$

where \underline{I} is the identity matrix.

Non trivial solutions occur at the resonance frequencies ω_ν , $\nu=1,2,\dots$, determined by the resonance condition

$$\det \underline{R} = 0 = \det (\bar{\Gamma} - \bar{\Gamma}^{-1}) \quad \text{at } \omega = \omega_\nu. \quad (7)$$

Because of radiation damping at the open end, the roots ω_ν are complex, with $\text{Im} \omega_\nu < 0$. Since this leads to exponentially growing elements in the matrix $\bar{\Gamma}$ (see Sec. 5.A 4 for the analytic continuation of κ_n and thereby of $\bar{\Gamma}$), the second form in (7), with $\bar{\Gamma}^{-1}$ denoting the inverse matrix, has computational advantages. The eigenvectors \underline{V}_ν^\pm , which define the self-consistent mode combination in the ω_ν resonance field, can be chosen as

$$\underline{V}_\nu^+ \text{ or } \underline{V}_\nu^- = \bar{\Gamma}_\nu \underline{V}_\nu^+ , \bar{\Gamma}_\nu \equiv \bar{\Gamma}(\omega_\nu) \quad (8)$$

The preceding format can now be built into a formulation for the scattered field u^s excited by a time-harmonic incident field u^i . Recalling that the modal expansion allows for *all* multiple interaction mechanisms ($\bar{\Gamma}$ contains internal as well as external contributions), one may write, with coordinate designation suppressed for simplicity,

$$u^s = Du^i + \underline{C}^t \underline{V}^- \quad (9)$$

where D is a scalar function which includes *all single scatter* field contributions at the observer (direct scattering from edges, single reflections, etc.). All multiple scatter contributions arise from the second term in (9), where \underline{C}^t is a transposed (i.e. row) vector whose functional elements express the conversion into the radiation field of a *unit* amplitude n^{th} modal field propagating toward the open end of the waveguide. The actual modal amplitudes with

$$\underline{V}^+ = \underline{B} u^i + \bar{\Gamma} \bar{\Gamma} \underline{V}^+ , \quad (10)$$

are synthesized by the *direct* excitation, due to u^i , of the modes propagating *into* the waveguide, with the column vector \underline{B} containing the *corresponding conversion* coefficients, and by the multiple interactions between the closed and open ends of the guide in the second term in (10) (which also accounts through $\bar{\Gamma}$ for all the external interactions). The two sets of equations (9) and (10) have a form analogous to Eqs. (8a) and (8b) in [8]. Combining them leads to the collective form for the scattered field

$$\underline{V}^+ = \underline{R}^{-1} \underline{B} u^i \quad (11)$$

$$u^s = \underline{C}^t \bar{\Gamma} \underline{R}^{-1} \underline{B} u^i + Du^i \quad (12)$$

The inverse matrix $\underline{R}^{-1} = \underline{R}^\dagger / \det \underline{R}$, where \underline{R}^\dagger is the adjoint matrix, can be expanded in terms of the (resonant) eigenvectors \underline{V}_ν^+ or \underline{V}_ν^- in (8), which correspond to the resonant frequencies ω_ν in (7). This permits (12) to be expressed in the form

$$u^s = Du^i + \sum_\nu \frac{\underline{a}^t \underline{B} u^i}{\frac{d}{d\omega} \det \underline{R}} \bigg|_{\omega_\nu} \frac{\underline{C}_\nu^t \underline{V}_\nu^-}{\omega - \omega_\nu} \quad (13)$$

where $\underline{C}_\nu^t \equiv \underline{C}^t(\omega_\nu)$ while the transposed vector \underline{a}^t is obtained from the Gauss elimination of the singular matrix $\underline{R}(\omega_\nu)$.

The series over ν in (13) represents the SEM expansion of the scattered field u_s , augmented by the direct scattering term Du^i (the *intrinsic entire function* [8]), which cannot be incorporated into the resonance series. The strength of each resonant contribution to u^s is determined by the "coupling coefficients" [7] $\underline{a}^t \underline{B}$ and \underline{C}_ν^t , which

project the resonant field structure of the target onto the incident and scattered fields, respectively.

Since the resonant fields are expressed in terms of the waveguide cavity resonances, the scattered field in (13) has been parametrized around the more prominent (high-Q) observables pertaining to the interior portion of the target, with the observables pertaining to the exterior portion included indirectly through the corresponding loading of the reflection matrix $\bar{\Gamma}_\nu$. By an alternative approach emphasizing the *external* observables, one may express the external interactions involving the edges $j=1$ to 4 self-consistently, and load the external scattering coefficients for edges $j=1,2$ by the collective coupling to the interior field. Either procedure generates the same resonance frequencies ω_ν , but a different eigenvector structure for the resonant fields.

ii. Partial resonance formulation

Although the global resonance formulation includes *all* ray field interactions between reflection and diffraction centers, these interactions have been grouped so as to distinguish between interior and exterior effects, as noted in the preceding paragraph. By decoupling the external from the internal contributions, one may highlight each through the corresponding *partial* resonances. Decoupling for the internal partial resonances is achieved by omitting effects due to edges $j=3,4$ in $\bar{\Gamma}$, while decoupling for the external partial resonances is achieved by omitting internal contributions to the $j=1,2$ diffraction coefficients. The global formulation is recovered by coupling the partial internal and external formulations.

Proceeding further along these lines, one may define partial resonances for the interior problem alone by ignoring some or all of the intermode coupling at edges $j=1,2$ as incorporated in the matrix $\bar{\Gamma}$ (it may be recalled from (4) that intermode coupling is identically zero in $\bar{\Gamma}$). Ignoring all intermode coupling implies that $\bar{\Gamma}_{nm} = 0$, $n \neq m$, so that (7) reduces to the partial resonance condition

$$\bar{\Gamma}_{nn} \bar{\Gamma}_{nn} = 1 \quad \text{at } \omega_\nu = \omega_{n,p}, \quad p = 1,2,\dots \quad (14)$$

where the index p tags the resonance solutions pertaining to the n -th waveguide mode. These partial resonances yield a good parametrization if they furnish good approximations to the global field structure. It is expected that this is indeed the case for the high-Q global resonances, which are found to occur near the n -th mode cutoff frequencies. Verification will have to be established by numerical experiment.

Similar partial resonance decompositions can be performed for the exterior problem, for example, by including all interactions between edges $j=2,3$ and $j=1,4$, while ignoring some or all between edges $j=3,4$. Because of the strong radiation damping, which accompanies each edge diffraction, it is impractical to carry out the external resonance construction. Instead, it is expected to treat the external effects by tracking a few multiple ray field interactions.

3. Construction of the Mode Reflection and Coupling Coefficients

i. Internal contributions

Here, contributions due to external interactions with edges $j=3,4$ are ignored, thereby rendering the internal contributions identical with those for the canonical infinite open-ended parallel plane waveguide. The canonical problem has been solved exactly by integral transform techniques [38], and asymptotically, in the high frequency domain, by ray techniques for modes not too close to cutoff [39-41], and by approximate transform techniques for modes near cutoff [31]. We shall concentrate on the asymptotic approach because it leads to a simpler form for the modal reflection coefficients (it shall be understood that mode "reflection" implies reflection into the same mode as well as coupling to other modes), and also because it generalized more readily to non-plane parallel configurations. Moreover, the asymptotic solution is readily continued into the lower half of the complex ω -plane where the resonances are located. It could be argued that overall consistency requires asymptotic treatment of the internal effects because the external effects, when included, can only be computed asymptotically. However, asymptotic consistency, to a given order in $(1/k)$, should not be imposed a priori because a more accurate treatment, not warranted for weak interactions, may yield better results and insight for a set of dominant interactions.

By the ray approach to mode reflection, diffraction of the incident modal congruences at edges 1 and 2 is followed by a succession of multiple diffractions between these edges before the ray field of the last interaction gets back into the waveguide; the multiple ray reflections inside the waveguide are treated collectively to synthesize the reflected modal fields. This process has been formalized in [39] to yield the following result for the coupling coefficient $\bar{\Gamma}_{mn}$ (see (5)) from an incident mode n to a reflected mode m ,

$$\bar{\Gamma}_{mn} = (\pm i/4\kappa_m a)(\epsilon_m/\epsilon_n)[1+(-1)^{m+n}]f(\theta_m, \theta_n) \quad (15)$$

where here and henceforth, upper and lower signs correspond to TM or TE polarization, respectively, and $\epsilon_n = 1$ or $\epsilon_n = 2$ for $n=0$ or $n \geq 1$, respectively. From (15) one finds that even and odd modes are uncoupled.

The edge diffraction pattern functions $f(\theta_m, \theta_n)$ is synthesized by the multiple diffraction process mentioned previously. Because the second and higher order diffractions take place along the reflection shadow boundary of the preceding diffraction, the interactive ray fields must be treated by uniform asymptotics, [40,41], which improves the earlier results in [39]. This solution can be expressed as follows:

$$f(\theta_m, \theta_n) = D(\theta_m, \theta_n)L_+(\kappa_m)L_+(\kappa_n) \quad (16)$$

where

$$\theta_j = \sin^{-1}(j\pi/ka) \quad (17)$$

with $j=m$ or n , is the modal angle of the j -th mode,

$$D(\theta_m, \theta_n) = -\sec(\theta_m - \theta_n) / 2 \mp \sec(\theta_m + \theta_n) = \mp 2 \sqrt{k \pm \kappa_m} \sqrt{k \pm \kappa_n} / (\kappa_n + \kappa_m) \quad (18)$$

is the edge diffraction coefficient, and, for $\kappa_j \neq 0$,

$$L_+ = 1 - (-1)^j K_j e^{ika} + (K_j^2 / 2! - K_j / 2^{3/2}) e^{2ika} - (-1)^j (K_j^3 / 3! - K_j^2 / 2^{3/2} + K_j / 3^{3/2}) e^{3ika} + \dots \quad (19)$$

with

$$K_j = e^{i\pi/4} (2\pi ka)^{-1/2} (k/\kappa_j) \quad (20)$$

In (19) we have retained only four terms that correspond to direct diffraction at the edges plus the first three interactions across the open end.

As has been shown in references [40,41], the function L_+ in (19) is the asymptotic approximation of an exact function $L_+(\kappa_j)$ that renders the expression in (16) exact. The exact function $L_+(\kappa)$ is used to factorize the function $[1 \mp \exp(ia\sqrt{k^2 - \kappa^2})]$ for the symmetrical or antisymmetrical even or odd j , respectively, in the Wiener-Hopf analysis of reflection from open-ended parallel plate waveguide. This function is given by $L_+(\kappa) = \exp U(\kappa/k, ka)$ or $\exp V(\kappa/k, ka)$ for the symmetrical or the antisymmetrical problem, respectively, where U and V are Weinstein functions defined in eqs. (10.07) and (10.18) in [42]. By numerical comparison of the asymptotic ray-optical result and the exact solution, one finds that the asymptotic form is accurate for both propagating and evanescent modes. However, from (15) with (16) and (19), the reflection coefficient diverges as $\kappa_j \rightarrow 0$, $j = n, m$. The transition function for $\kappa_j \simeq 0$, as obtained by Weinstein [42,43], is given by

$$L_+(\kappa_j) = \kappa_j \sqrt{2a/k} \exp \left[\frac{1}{2} (i-1) \beta \kappa_j \sqrt{a/k} - i\pi/4 \right] \quad (21)$$

where $\beta = \zeta(1/2) / \sqrt{\pi} = 0.82391$ and ζ is the Riemann zeta function.

ii. External contributions

The external contributions arise from single and multiple diffracted ray fields involving edges 1 to 4, and terminating at edges 1 and 2 before diffracting back into the waveguide. These interactions can be treated collectively in their totality or in part to synthesize global or partial external resonances, respectively. Because of the substantial radiation losses at each diffractions, these resonances are strongly damped relative to the higher-Q internal resonances. Therefore, as argued in [44] and verified by numerical comparison in Section III, the external loading of the higher-Q internal resonances is minimal, and can be accounted for adequately by retention of a few ray interaction events. Therefore, only the dominant interactions $j=1-4-1$ and $j=2-3-2$ have been taken into account, with the corresponding contribution

$$f_c(\theta_m, \theta_n) = G_o^2(L) D(2\pi, \theta_n) D(\theta_m, 2\pi) D_{\pi/2}(0, 0) \quad (22)$$

where $G_0(L) = (8\pi kL)^{-1/2} \exp(ikL + i\pi/4)$ is the normalized GTD propagator between the edges in question, D is the half plane diffraction coefficient in (16a), and $D_{\pi/2}$ is the diffraction coefficient for a wedge 90° internal angle [45]. This external pattern function can be added to the internal function (16), thereby generating external loading of the internal effects, or it can be treated individually to furnish the external-internal coupling. The internal coupling, in turn, can proceed directly from edges $j=1$ and 2 , respectively (first term inside the braces in (16)), or with inclusion of diffractions across the open end, as expressed by the remaining terms in (16).

4. Extension into the Complex Frequency Domain

Since, for the $\exp(-i\omega t)$ dependence assumed here, the relevant portion of the complex frequency plane for describing the resonance and other transient phenomena in $\text{Im } \omega \leq 0$, it is necessary to continue the expressions for the various wave objects defined in the preceding sections into this complex domain. The analytic continuation of the exact edge diffraction pattern function in (16) with the exact function L_+ is presently unknown. However, the analytic extension of the approximate expressions using the function L_+ from either (19) or (21) is direct and requires only the proper definition of the multivalued functions (a) $k^{1/2}$ in (20), (b) $\kappa_n = (k^2 - k_{xn}^2)^{1/2}$ and (c) $(k \pm \kappa_n)^{1/2}$ in (18). All functions have already been defined to be positive (when real) for positive real k . This allows their unique analytic continuation into the multibranch k -plane, subject to the choice of branch cuts. For (a), we choose a branch cut extending from $k=0$ to infinity along the negative imaginary axis. For (b), we choose a cut extending along the real k -axis from $(-k_{xn})$ to $(+k_{xn})$ so that $\text{Im } \kappa_n < 0$ in the lower half of the ω -plane; this also defines indirectly the analytic continuation of (c). A numerical comparison, for $\text{Im } \omega \geq 0$, of the exact function L_+ with the approximated functions in (19) and (21) has revealed that the ray optical formula (19) may be used for $|\kappa_j| > \sqrt{k/\pi a}$, whereas near the cutoff frequency of the j -th mode, one should use (21).

5. Numerical Results

Numerical implementation of the radar cross section algorithm in (13) has been initiated. Initial emphasis has been placed on testing the partial vs. global resonance descriptions detailed in Sections 1 and 2. This involves solving the internal partial resonance equations for individual internal modes, solving the external partial resonance equations, etc., and then repeating by allowing for selected couplings between these individual effects to generate modified partial resonances. The various partial resonances are then to be compared with the fully coupled global resonances to identify the features that partial resonances explain well. The role played by evanescent modes in the coupled case requires special attention, and certain subtleties in this connection, especially for the more strongly damped resonances, will also receive attention.

The numerical calculations involve a waveguide length-to-width ratio $L/a=5$, and asymmetrical TM_n modes ($n=1,3,5,\dots$). Thus, there is no coupling to TM_n modes with n even. Since the resonance map in the lower half of the (normalized) complex (ka) plane is symmetric about the imaginary axis, only the fourth quadrant is shown. The frequency window has been restricted to $\text{Re}(ka) \leq 20$, thereby eliminating the propagating modes to $n=1,3,5$. Modes with $n \geq 7$ are evanescent.

Preliminary results for the partial resonances in (14) attributed to the internal TM_n mode resonances $n=1,3,5$ are plotted in Fig. 5. The resonances are arranged in layers (n,p) , where n identifies the layer and p position inside the layer. External coupling has been omitted and included, and reflection at the open end has been modeled by single and multiple edge diffraction as expressed by the various terms inside the braces in (19). Also shown in Fig. 5 are the external resonances, decoupled from the internal ones. The external resonances have been determined from the roots of the flow graph determinant, following the procedure in [8].

The n -th mode individual resonance layer is seen to start with the least damped resonance near the n -th mode cutoff frequency $\text{Re}(ka) = n\pi$. At frequencies near modal cutoff, the ray optical formula for the modal reflection coefficient diverges (cf. [39-41]), with a resulting error in the location of the near-cutoff resonances (small p), which are found to lie incorrectly in the *upper* half of the complex ω -plane. The correct results in these frequency windows, shown in the insets in Fig. 5, are found using the transitional form of L_+ in (21). At frequencies away from modal cutoff, the ray optical formula is valid, and the corresponding (large p) results are correct. Certain basic features of the partial resonances as described below. The near-cutoff resonances have high Q because diffraction losses at the open end are minimized by the nearly vertical propagation direction (with $\kappa_{n,p} \approx 0$) of the corresponding wave spectra, as expressed by the propagation vectors $k_{n,p}^{\pm} = \pm \hat{x} n\pi/a - \hat{z} \kappa_{n,p}$, where \hat{x} and \hat{z} are unit vectors along x and z . The wave tilt is such as to accommodate approximately a longitudinal quarter-wavelength $\lambda_{z_n} \approx 2\pi/\text{Re}(\kappa_{n,p})$ over the cavity length L . As $\text{Re}(ka)$ increases away from cutoff, λ_{z_n} decreases, and resonances $p > 1$ may be found which correspond to

$$L/\lambda_{z_{n,p}} \approx \frac{1}{2}p - \frac{1}{4}, \quad p = 1, 2, \dots \quad (23)$$

These resonances have lower Q because of higher edge diffraction losses attributable to the more oblique wave spectra. Eventually, when $\text{Re}(ka)$ is sufficiently large so that $\kappa_{n,p} \gg n\pi/2$, the wave spectra are nearly horizontal, and therefore experience approximately the *same* diffraction losses, for various p . This causes the resonances to stabilize around an asymptotic $\text{Im}(ka)$ value, with approximate $\text{Re}(ka)$ values that correspond to $\lambda_{n,p} \approx \lambda_{z_{n,p}} \approx 2L/p$, where $\lambda_{n,p}$ is the free space wavelength. Thus, the small- p resonances convey information, essentially, about the waveguide plate spacing a , while the large- p resonances convey information about the waveguide length L .

The resonances are affected, of course, by the modeling of the open end diffraction. When multiple diffraction between edge 1 and edge 2 in Fig. 1 is ignored, the layer contour slope is monotonic (Fig. 5). When one or more multiple diffractions are taken into account (see (19)), the contour shows kinks near $\text{Re}(ka)$ values corresponding to the cutoff frequencies of the higher order modes, with small differences in resonance location between including two diffractions (not shown in Fig. 5) and three diffractions, and with no noticeable difference in shape by including four or more interactions. Therefore, reflection has been modeled by retaining up to triple diffraction. Multiple diffraction evidently conveys additional information about the waveguide height a via the higher mode cutoff perturbation.

The antisymmetric external resonances generate a low Q layer and, when coupled to the internal modes, perturb the TM_n resonances only slightly (see Fig. 5 for the TM_1 mode perturbation). In fact, the external loading of the internal resonances is found to be adequately expressed by the few dominant ray interactions in (22).

Calculation of the corresponding eigenvectors (see (8)), of similar results allowing for selected mode coupling, and of the global resonances accounting for *all* interactions, is in progress.

B. Hybrid (Ray-Mode)-(Boundary Element) Method for Wave Scattering from Aperture Coupled Systems*

This study involves a new method which combines the hybrid ray-mode and boundary element methods. The latter is used to formulate the aperture scattering process and the former to provide the Green's function of the layered environment. Following the standard procedure of the boundary element method [1], we first formulate integral equations for the field distribution across the aperture. By expressing this unknown distribution in terms of appropriate basis functions, the integral equations are then reduced to algebraic equations which are solved numerically. In the integral equations, one needs to compute the Green's function of the internal environment for various arrangements of locations of source and receiver. None of the conventional approaches (rays, modes and spectral integration) is satisfactory to evaluate the Green's function for all possible arrangements. The newly developed hybrid ray-mode method [11,22,24] is best suited for this purpose because it combines rays and modes self-consistently within a single framework and optimizes the advantage of each.

To test this approach, we have chosen a simple prototype structure, similar to the one in Section A, for which the various constituents in the analysis can be treated with

(*) This phase is being worked on by I-T. Lu and B. Ma.

good accuracy and without undue complication. The configuration involves a perfectly conducting, thin-walled plane parallel waveguide whose interior is coupled to the exterior by an infinitely long slit of large width in one of the walls (Fig. 6). The interaction will be analyzed by the (GTD-ray)-mode parametrization as for the problem in Section A, but generalized to include the *hybrid* ray-mode scheme for the *interior*. The interaction will also be analyzed by the moment method applied to the aperture field, with the above-described coupling to the hybrid waveguide Green's function. This will furnish the numerical reference solution. Although the moment method is efficient only for moderate slit width (in terms of wavelength), there will be a region of overlap with the lower end of the high-frequency asymptotic ranges that are best suited to the GTD ray approach.



Fig. 6 Perfectly conducting, thin-walled plane parallel waveguide with an infinitely long slit in one of the walls.

Thereafter, following the procedure in [18], wherein GTD methods were applied to constructing the complex resonances for a slit in an infinite plane boundary, the new approach described above will be used to account for the changes in the resonance behavior of the slit when the environment on one side is the plane parallel waveguide.

After these fundamental studies will have been completed, the new (ray-mode)-(boundary element) method will be applied to the more complex configurations shown in Fig. 2.

At the present stage of this investigation, the formulation of the problem has been completed, and numerical implementation is being initiated. The GTD-mode scheme will be considered soon.

C. Slit-Coupled Convex Perfectly Conducting Thin Cylindrical Shell with Interior Convex Perfectly Conducting Cylindrical Loading*

This configuration, which generalizes the one schematized in Fig. 2, to noncircular shapes, is being investigated via the external-ray and internal-local mode format. The analysis embodies a substantial generalization of that for the problem in Section A.

First consideration has been given to the appropriate parametrization of the scattering problem. When the interior load has dimensions approaching those of the enclosing shell, a waveguide with variable cross section is formed along the interior peripheral direction. This requires treatment via local modes, which may undergo cutoff at narrow portions. On the outside, the treatment is via creeping rays. The slit is assumed to be narrow, thereby localizing its scattering properties and endowing the interior cavity resonances with *high Q*. The formulation suited to this model has been carried out via a system of state vectors, propagation matrices and coupling matrices that tie the hybrid ray-mode constituents together self-consistently. Reduced simplified alternative parametrizations of the scattering problem have also been considered, which emphasize the different parameter regimes away from, or near, an interval resonance, respectively.

The near-resonance problem is the most difficult. Pursuit of a perturbation scheme is in progress, which seeks to predict the location of the resonance spikes in the *bistatic scattering cross section* from the resonances of the closed asymmetrically loaded cavity and the slit coupled symmetrically loaded cavity.

6. REFERENCES

1. C.A. Brebbia, *The Boundary Element Method for Engineers*, Wiley, New York, 1978.
2. V.K. Varadan and V.V. Varadan (editors), *Acoustic, Electromagnetic and Elastic Wave Scattering - Focus on the T-Matrix Method*, Pergamon Press, New York, 1980.

(*) This phase is being worked on by L.B. Felsen and G. Vecchi.

3. M.H. Schultz and D. Lee (editors), *Computational Ocean Acoustics*, Pergamon Press, New York, 1985.
4. K.M. Chen, D.P. Nyquist, E.J. Rothwell, L.L. Webb and B. Drachman, "Radar Target Discrimination by Convolution of Radar Return with Extinction Pulses and Single-Mode Extraction Signals," *IEEE Transactions Antennas Propagat.* AP-34, (1986), pp. 896-904.
5. D.G. Dudley, "Comments on SEM and the Parametric Inverse Problem," *IEEE Trans. Antennas Propagat.*, AP-33, (1985), pp. 119-120.
6. L.W. Pearson, "A Note on the Representation of Scattered Fields as a Singularity Expansion," *IEEE Trans. Antennas Propagat.*, Vol. AP-32, (1984), pp. 520-524.
7. M.A. Morgan, "Singularity Expansion Representations of Fields and Currents in Transient Scattering," *IEEE Trans. Antennas Propagat.*, vol. AP-32, (1984), pp. 466-473.
8. E. Heyman and L.B. Felsen, "A Wavefront Interpretation of the Singularity Expansion Method," *IEEE Trans. on Antennas and Propagation*, AP-33, (1985), pp. 706-718.
9. L. B. Felsen, "Comments on Early Time SEM", *IEEE Trans. Antennas Propagat.* AP-33, 118-19, 1985.
10. For a representative collection of basic papers on GTD, see R.C. Hansen (editor), *Geometric Theory of Diffraction*, IEEE Press, New York, 1981.
11. L.B. Felsen, "Progressing and Oscillatory Waves for Hybrid Synthesis of Source Excited Propagation and Diffraction," Invited Paper, *IEEE Trans. on Antennas and Propagation*, AP-32, (1984), pp. 775-796.
12. L. B. Felsen, "Novel Ways for Tracking Rays", Invited Paper, *J. Opt. Soc. Am. A2*, (1985) pp. 954-963.
13. L. B. Felsen, "Real Spectra, Complex Spectra, Compact Spectra, *J. Opt. Soc. Am. A*, Vol. 3, No. 4, April 1986.
14. L. B. Felsen, "Target Strength: Some Recent Theoretical Developments," *IEEE Journal of Ocean Engineering*, QE-12, pp. 443-452, 1987.
15. J. M. Arnold and L. B. Felsen, "Local Intrinsic Modes--Layer with Non-planar Interface," *Wave Motion* 8 (1986), pp. 1-14.
16. E. Topuz and L. B. Felsen "Sound Pulse Propagation in a Weakly Range Dependent Shallow Ocean, to be published in *Proceedings of the Symposium on Ocean Seismo-Acoustics*, held in LaSpezia, Italy, June 1985.
17. P. D. Einziger and L. B. Felsen, "Rigorous Asymptotic Analysis of Transmission through a Curved Dielectric Slab," *IEEE Trans. on Antennas and Propagation*, Vol. AP-31, No. 6, November 1983, pp. 863-870.

18. ** H. Shirai and L. B. Felsen, "Modified GTD for Generating Complex Resonances for Flat Strips and Disks", IEEE Trans. on Antennas and Propagation, AP-34, No. 6, June, 1986, pp. 779-790.
19. E. Heyman and L.B. Felsen, "Traveling Wave and SEM Representations for Transient Scattering by a Circular Cylinder," J. Acoust. Soc. Am. 79, (1986) pp. 230-240.
20. H. Shirai and L.B. Felsen, "Wavefront and Resonance Analysis of Scattering by a Perfectly Conducting Flat Strip," IEEE Trans. on Ant. and Propagat., ASP-34, pp. 1196-1207, 1986.
21. H. Ikuno and L.B. Felsen, "Complex Ray Interpretation of Reflection from Concave-Convex Surfaces," submitted to IEEE Transactions Antennas and Propagat.
22. I.T. Lu and L.B. Felsen, "Ray, Mode and Hybrid Options for Transient Source Excited Propagation in an Elastic Layer," Geophys. J. Roy. Astron. Soc. 86, (1986), pp. 177-201.
23. I-Tai Lu, L.B. Felsen and J.M. Klosner, "Hybrid Beam-Mode Formulation of QNDE in Layered Media," In preparation.
24. H. Shirai and L.B. Felsen, "Rays, Modes and Beams for Plane Wave Coupling into a Wide Open-Ended Parallel Waveguide", to be published in Wave Motion.
25. V. Cerveny, "Ray Synthetic Seismograms for Complex Two-Dimensional and Three-Dimensional Structures," J. Geophysics 58, (1985), pp. 2-26.
26. V. Cerveny, "Ray Synthetic Seismograms for Complex Two-Dimensional and Three-Dimensional Structures," J. Geophysics 58, (1985), pp. 44-72.
27. P.D. Einziger, Y. Haramaty and L.B. Felsen, "Complex rays for radiation from discretized aperture distributions," J. Opt. Soc., A, Apr. 1986.
28. P.D. Einziger, Y. Haramaty and L.B. Felsen, "Complex Rays for Radiation from Discretized Aperture Distributions", to be published in IEEE Transactions on Antennas and Propagation.
29. L. B. Felsen, "Complex-Source-Point Solutions of the Field Equations and Their Relation to the Propagation and Scattering of Gaussian Beams", Symposia Matematica, Instituto Nazionale di Alta Matematica, Vol. XVIII, Acad. Press,

(*) These papers received the 1984 R.W.P. King Best Paper Award from the IEEE Antennas and Propagation Society.

(**) This paper received the 1987 R.W.P. King Best Paper Award from the IEEE Antennas and Propagation Society.

- London and New York, 1976, pp. 40-56.
30. S. Y. Shin and L. B. Felsen, "Gaussian Beam Modes by Multipoles with Complex Source Points", *J. Opt. Soc. Am.*, **67**, No. 5, May 1977.
 31. L. B. Felsen, "Geometrical Theory of Diffraction, Evanescent Waves, Complex and Gaussian Beams", *Geophys. J. Roy. Astron. Soc.*, (1984) **79**, pp. 77-88.
 32. Y. Z. Ruan and L. B. Felsen, "Reflection and Transmission of Beams at a Curved Interface", *J. Opt. Soc. Am. A*, Vol. 3, No. 4, April, 1986.
 33. I. T. Lu, L. B. Felsen, Y. Z. Ruan and Z. L. Zhang, "Evaluation of Beam Fields Reflected at a Plane Interface, to be published in *IEEE Trans. on Ant. and Propagat.*
 34. I.T Lu, L.B. Felsen and Y.Z. Ruan, "Spectral Aspects of the Gaussian Beam Method: Reflection from an Isovelocity Half Space", to be published in *Geophys. J. Roy. Astron. Soc*
 35. R.W. Ziolkowski, "New Electromagnetic Effects Associated with Cavity-Backed Apertures," paper presented at *URSI International Symposium on Electromagnetic Theory*, Budapest, Hungary, August 1986.
 36. I.T. Lu and L.B. Felsen, "Adiabatic Transforms for Spectral Analysis and Synthesis of Weakly Range Dependent Shallow Ocean Green's Function," *J. Acoust. Soc. Am.*, **81**(4), pp. 897-911, Apr. 1987.
 37. I.T. Lu and L.B. Felsen, "Range Dependent Canonical Solutions for Shallow Ocean Acoustics," to appear in the *Proc. IMACS Symp. on Computational Acoustics at Yale University*.
 38. B. Noble, "Methods Based on the Wiener Hopf Technique for the Solution of Partial Differential Equations," Pergamon Press, 1958.
 39. H.Y. Yee, L.B. Felsen and J.B. Keller, "Ray Theory of Reflection from the Open End of a Waveguide," *SIAM J. Appl. Math.*, Vol. 16, pp. 268-300, 1968.
 40. J. Boersma, "Ray Optical Analysis of Reflections in an Open-Ended Parallel Plane Waveguide: I - TM Case," *SIAM J. Appl. Math.*, Vol. 29, pp. 164-195, 1975.
 41. J. Boersma, "Ray Optical Analysis of Reflection in an Open-Ended Parallel Plane Waveguide: II - TE Case," *Proc. IEEE*, Vol. 62, pp. 1475-1481, 1974.
 42. L.A. Weinstein, "The Theory of Diffraction and the Factorization Method," P. Beckmann tr., Golem Press. Boulder, CO, 1969.
 43. L.A. Weinstein, *Open Resonators and Open Waveguides*, P. Beckman tr., Golem Press, Boulder, CO, 1969.
 44. E. Heyman, "The Hybrid Wavefront Resonance Method," in *Theoretical Aspects of Target Classification*, L.B. Felsen, Ed., AGARD-LS-152, AGARD, Neuilly-

sur-Seine, France, 1987.

45. R.G. Kouyoumjian, "The Geometrical Theory of Diffraction and its Applications," in *Numerical and Asymptotic Techniques in Electromagnetics*, R. Mittra ed., Springer Verlag, NY, 1975.

B. MICROPARTICLE PHOTONICS

Professor S. Arnold, K.M. Leung, and L.M. Folan

Unit EM8-2

1. OBJECTIVE(S)

The main goal of this project is to investigate both experimentally and theoretically the intrinsically nonlinear interaction of intense electromagnetic waves with three-dimensional optically nonlinear structures whose refractive indices are functions of the intensity of the local electric field. These structures can have sizes which are small or large when compared with the wavelength. Our research program will first be directed to the study of isolated structures with well-defined geometries. The results will then be extended to include collections of these microstructures either randomly distributed in a gaseous environment or embedded in regular arrays inside a transparent host medium. Our aim is to understand, on one hand, the limitations on the performance of electromagnetic systems due to scattering and absorption by particles suspended along the propagation path, and on the other, to establish a new approach to nonlinear electromagnetic problems, with a view towards developing a whole new class of optical devices and a new discipline, best called microparticle photonics.

2. SUMMARY OF RECENT PROGRESS

In this section we will review our recent progress since April, 88 when this contract started. A number of areas of progress associated with Microparticle Photonics will be briefly discussed. In the next section each of these advances will be elaborated on in greater detail.

We have attacked the problem of nonlinear 3-D structures by imagining a sphere to be the basic building block. Since the general nonlinear solution for the EM fields within such a structure is unknown, except for the limiting case of a Rayleigh particle [1], experimental data on such structures are paramount. In this regard we would particularly like to know the strength to which the EM fields can grow in a spherical dielectric structure. Since the maximum strength of the electric field is proportional to the quality factor at a so-called Morphologically Dependent Resonance (MDR), Q , we first attempted to determine the largest quality factor obtainable. Here we were aided by a recent theory in the literature in which the degree of intermolecular energy transfer within a spherical structure is related to the quality factor of various MDR's [2]. Our recent experiments have confirmed this theory and allowed us to estimate the photon lifetime within the longest lived resonances of a particle 10 nm in radius. The corresponding Q within these modes was found to be 4.4×10^6 [3]. This *unprecedented value for the room temperature quality factor* suggested that incident intensities needed to produce nonlinear behavior could be extremely small. To further

take advantage of this situation a "so-called" artificial Kerr medium [4] consisting of Rayleigh-sized particles (60 nm in diameter) which are free to move within a Mie-sized particle was constructed. *The addition of these small particles was found to produce optical bistability at the extremely small intensity of 1200W/cm².* As we will see in the next section this bistability may be understood in terms of a change in the refractive index profile within the particle caused by intensity dependent gradient forces. The artificial Kerr medium is by no means ideal due to its slow response, however, it is a good model system because of the relatively large effective nonlinear Kerr coefficient n_2 [i.e., with the refractive index expressed as $n = n_0 + n_2 I$, n_2 values 10^5 times the value for CS₂ have been measured] and thus experiments can be made using low power CW lasers. In order to advance to faster materials which are analogous to the liquid drops which we have been using, we have begun to construct nonlinear glass spheres by utilizing a new device developed in our laboratory known as a Convective Oven. With this technique in hand we are able to fabricate glass spheres of a number of different materials. Perhaps the most interesting of these materials are filter glasses with large values of n_2 . These glasses are attractive media for such devices since recent work has shown that relatively large nonlinear coefficients are possible while still maintaining response times below 100fs [5]. In fact an all optical nonlinear fiber coupler switch recently constructed by P.W. Smith and his group at Bell Communication Research [6] has already proven to be the fastest optical fiber switch known [7]. While examining amorphous media at the Polytechnic, we have entered into a collaboration with the A. Pluchino and his group at the Aerospace Corp. where work is currently underway on spherical particles which are composed of traditional semiconducting materials. Although single crystals of these materials have larger nonlinearities than glass, our semiconducting particles are polycrystalline and internal scattering losses tend to damp the normally high Q resonances. This aside, we have observed optical hysteresis in these particles, and this hysteresis currently occurs only near frequencies corresponding to MDR's of the semiconductor particles.

On the theoretical side we have calculated the effective nonlinear dielectric function of a mixture consisting of a random distribution of Rayleigh-sized microparticles. We assumed that the particles are made up of materials whose dielectric function depends on the local intensity. The results are rather general, and apply regardless of the particular form of dependence of the refractive index on the intensity. The main assumption is that the concentration of microparticles is small. We find that at low intensity, an effective Kerr coefficient for the mixture can be defined. At higher intensity, the effective nonlinear dielectric function of the composite can itself be a multi-valued function of the intensity. Specific results have been computed for the case of a Kerr-like material whose Kerr coefficient can be either positive or negative.

3. STATE OF THE ART AND PROGRESS DETAILS

The areas mentioned in Sec. 2 above are reviewed here in more detail.

(1) Measurement of the Quality factor of the highest Q modes of a Microparticle

The quality factor of the longest lived resonance of a spherical dielectric particle was estimated by the use of a new method based on the phenomenon of Microparticle Enhanced Energy Transfer (MEET) [8]. Here energy from an excited donor molecule is transferred to an acceptor indirectly. The donor molecule is stimulated by its interaction with high Q MDR's of the particle to deposit its energy in the particle. The photon so deposited remains in the particle until it is either absorbed by an acceptor molecule or leaks out. At an acceptor concentration at which absorption by acceptors far exceeds leakage, the energy transfer is independent of concentration (i.e., it saturates). However as the concentration of acceptors is reduced to the point at which absorption by acceptors is comparable to leakage the energy transfer falls to 1/2 of its saturation value. By determining this critical concentration one can obtain an estimate for the Q of the longest lived resonances. A quantum electrodynamic theory for the MEET process has recently been worked out by P.T. Leung and K. Young [2]. The concentration dependence predicted by theory is born out through our experiments. The largest Q value for a particle having a refractive index of $1.47 + 10^{-9}i$ and a radius of 10μ is 4.4×10^6 . Recently the largest quality factor for individual particles in a stream has been estimated by interpreting the delay between a picosecond pulse and the onset of Stimulate Raman Scattering (SRS) as equivalent to the photon lifetime [9]. Although there are no current calculations to support this notion, it is interesting to note that our Q factor is within a factor of 2 of that obtained from SRS experiments [9], and that both numbers fall short of the prediction from Mie theory by orders of magnitude. It is thought that photon coupling to mechanical modes associated with surface roughness is responsible for this effect. Our paper on the measurement of Q using the theory of Leung and Young is in press [3].

(2) Measurements on a Microparticle Containing an "Artificial" Kerr Medium

To address nonlinear problems we have given liquid droplets for which the linear physical characteristics are known (i.e. size, refractive index, quality factors of resonant modes) a pronounced nonlinear character. *Our interest at this point is in a model system, not a practical system.* Our means for doing this is through the generation of an artificial Kerr medium in which we take advantage of the motion of Rayleigh size particles in optical fields having intensity gradients.

A Rayleigh particle in an electromagnetic field in vacuum experiences a force in the direction of the gradient of the time averaged intensity. Thus the Rayleigh particle is pulled into regions of high intensity. In a condensed system such as a liquid containing a statistical number of particles, high local intensities will therefore produce a relatively large refractive index; the new medium (i.e., particles in liquid) acts as an "artificial" Kerr medium. If this Kerr medium fills a Mie particle, than the particle becomes a model system for a nonlinear 3D structure. More importantly it is a Kerr medium with a very large Kerr coefficient. Consequently one has the potential of experimenting on this structure with a low power CW laser without competition from other effects (e.g., thermal, etc).

We have done just such experiments on droplets $\sim 10\mu$ in radius in which as many as 10^3 - 10^4 Rayleigh particles 60 nm in diameter have been placed. Our current results are preliminary, however, these results show a clear optical bistability (OB) in the wavelength dependence of the elastic scattering. Further work is necessary to verify that the mechanism for this OB is entirely associated with n_2 and not a thermal effect [10].

(3) Semiconducting Particles

In collaboration with A. Pluchino of the Aerospace Corp. we have begun to perform experiments on semiconducting particles on glass substrates. In our first experiments on spherical CdS particles we have measured the intensity dependence of the elastic scattering from individual particles 1- 5μ in diameter. In all cases we find a pronounced optical hysteresis beyond a critical intensity. The associated wavelength dependence of this effect indicates that the effect is strongest near MDR's of the particle. Our present experiments have only been carried out to MHz frequencies, however, in the future these experiments will be extended to higher frequencies in order to separate effects which are thermal from those which are intrinsic.

(4) Theoretical Determination of the Effective Dielectric Function of an Inhomogenous Medium

The problem of determining the effective dielectric function of an inhomogenous medium given the properties of its constituents has been of interest for quite a long time. A number of theories are available in the linear regime, including the widely popular theories of Maxwell-Garnett [11], and Bruggeman [12]. In these theories it is assumed that the particles as well as the host medium both behave linearly. There is a recent work on the effective dielectric function of composite materials in the nonlinear regime [13]. In this work it was assumed that the dielectric function is periodic, with the period approaching zero. It was concluded that explicit computation of this function is in general impossible, even by numerical methods. In our work here, by extending the theory developed by Landau and Lifshits, we are able to obtain explicit result for the effective dielectric function for composite media. Our calculation relies on the results we obtained previously on the intrinsically nonlinear interaction of EM waves with single spherical Rayleigh-sized particles [1]. The real part of the nonlinear dielectric function of the composite is plotted as a function of the reduced incident intensity in Fig.1. It can be seen that an effective Kerr coefficient can be defined at low intensity from the slope of the curve near $q=0$. However, away from the low intensity region, it is clear that it is no longer possible to define such an effective Kerr coefficient. Dependence on higher powers of the intensity becomes so important that the effective dielectric function itself can become a multi-valued function of the intensity. This is a highly unusual result because in nonlinear optics, one almost always starts out with a dielectric function which is a single-valued function of the field, although under appropriate circumstances certain physical quantities may end up multi-valued. The origin of this anomaly clearly lies in the composite character of the mixture and that each nonlinear microparticle can individually exhibit optical

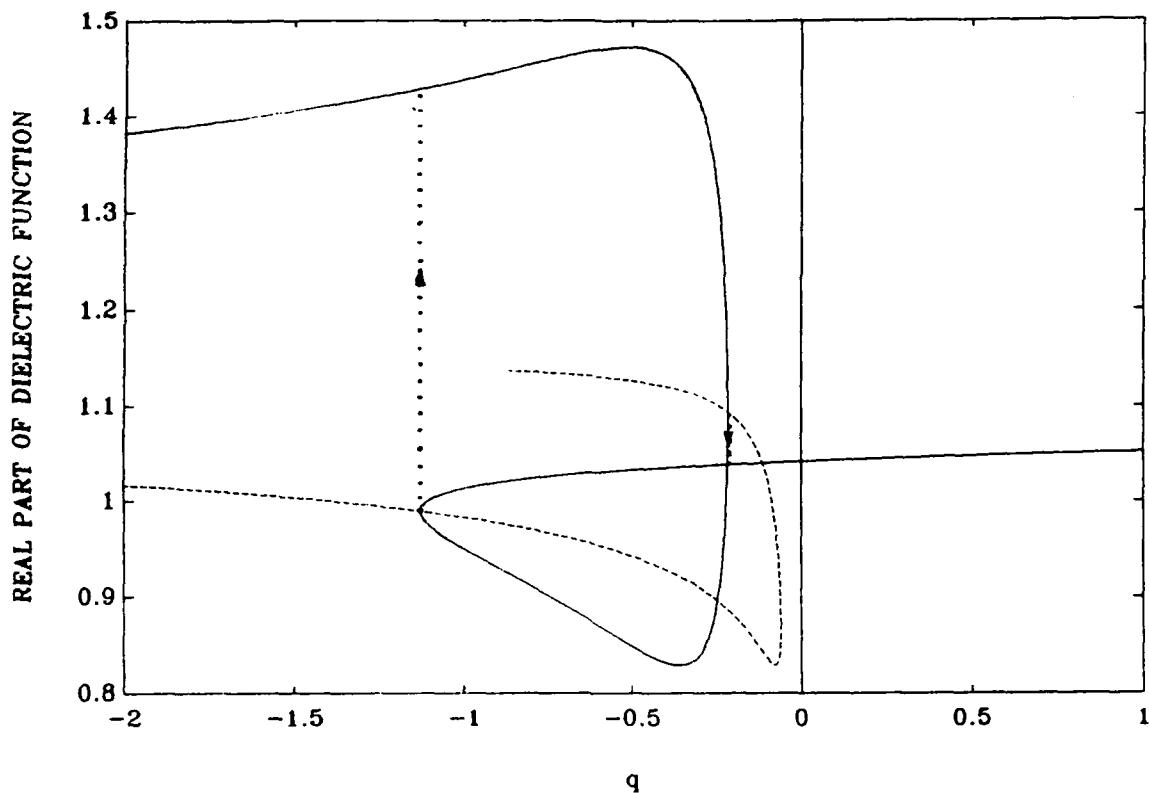


Fig. 1 The real part of the effective nonlinear dielectric function of a random distribution of spherical Rayleigh-sized microparticle embedded in a transparent host medium.

bistable behavior.

It is hoped that our work will enable us to better understand the manner in which intense EM waves interact and propagate through aerosols containing optically nonlinear microparticles. Our results can also be applied to give the effective dielectric function of glasses doped with optically nonlinear semiconductor microcrystallites. The use of such man-made materials in nonlinear optics has been attracting some attention in recent years [14]. In fact an experimental observation of optical bistability in $\text{CdS}_x\text{Se}_{1-x}$ doped glasses has recently been reported [15].

4. REFERENCES

1. K.M. Leung, "Optical Bistability in the Scattering and Absorption of Light from Nonlinear Microparticles", *Phys. Rev.A* 33, 2461 (1986).
2. P.T. Leung and K. Young, "Theory of Enhanced Energy Transfer in an Aerosol Particle", *J. Chem. Phys.* 89, 2894 (1988).
3. S. Arnold and L.M. Folan, "Energy Transfer and the Photon Lifetime within a Microparticle", *Opt.Lett.*(in press).

4. P.W. Smith, P.J. Maloney, and A. Ashkin, "Use of a Liquid Suspension of Dielectric Spheres as an Artificial Kerr Medium", *Opt. Lett.* **7**, 347 (1982).
5. I. Thomazeau, J. Etchepare, G. Grillon, and A. Migus, "Electronic Nonlinear Optical Susceptibility of Silicate Glasses", *Opt. Lett.* **10**, 223(1985).
6. S.R. Friberg, Y. Silberberg, M.K. Oliver, M.J. Andrejco, M.A. Saifi, and P.W. Smith, "Ultrafast All-optical Switch in a Dual-core fiber Nonlinear Coupler", *Appl. Phys. Lett.* **51**, 1135(1987).
7. P.W. Smith, Private Communication.
8. L.M. Folan, S. Arnold, and S.D. Druger, "Enhanced Energy Transfer within a Microparticle", *Chem. Phys. Lett.* **118**, 322-327 (1987).
9. Jian-Zhi Zhang, D.L. Leach, and R.K. Chang, "Photon Lifetime within a Droplet: Temporal Determination from Elastic and Raman Scattering", *Opt.Lett.* **13**, 270(1988).
10. S. Arnold, K.M. Leung and A.B. Pluchino, "The Optical Bistability of an Aerosol Particle", *Opt. Lett.* **11**, 800-802(1986).
11. J. C. Maxwell Garnett, *Philos. Trans. Roy. Soc.* **203**, 385 (1904); **205**, 237 (1906).
12. D. A. G. Bruggeman, *Ann. Phys. (Leipzig)*, **24**, 636 (1935).
13. G.C. Papanicolaou, *Electromagnetic Problems in Composite Materials in Linear and Nonlinear Regimes in Nonlinear Electromagnetics*, ed. by P. L. E. Uslenghi, p. 253 (Acad. P, N.Y., 1980).
14. K. C. Rustagi and C. Flytzanis, *Opt. Lett.* **9**, 344 (1984).
15. J. Yumoto, S. Fukushima, and K. Kubodera, "Observation of optical bistability in $\text{CdS}_x\text{Se}_{1-x}$ doped glasses with 25-psec switching time" *Opt.Lett.* **12**, 832 (1987).

C. BEAM-FIELD INTERACTIONS WITH NONLINEAR THIN FILMS

Professors K. Ming Leung and Theodor Tamir

Unit EM8-3

1. OBJECTIVES

The aim of this project is to investigate a new class of electromagnetic phenomena that involve *bounded beams* propagating under *nonspecular regimes* in the presence of planar *nonlinear media*. These phenomena are produced by the combination of (a) unexpectedly large nonspecular effects involving beams in thin films, with (b) the field-modification behavior of dielectric layers whose refractivity is intensity-dependent. The overall effects include beam displacements of the lateral, angular and longitudinal types, field focusing or fragmentation, as well as other varieties of field changes and beam distortions.

By exploiting the action of nonlinearities to enhance and modify the nonspecular effects, novel techniques for dynamically controlling beam trajectories can be explored. These techniques will thus be useful in the design of optical components and in the implementation of optoelectronic devices.

2. SUMMARY OF RECENT PROGRESS

During the past period, our investigation has considered two major aspects involving propagation of fields in or along nonlinear layers. First, we have studied the transmission of a homogeneous plane wave through Kerr-like media characterized by a negative nonlinearity. Specifically, our previous exact analytical study of the scattering of plane TE polarized waves from a nonlinear film has been extended to the case of films with a self-defocusing nonlinearity. The reflectivity and the internal field intensity were calculated as functions of the angle of incidence, the film thickness, and the incident intensity. All the possible allowed types of behavior were investigated and optical bistability in the reflectivity was found to be possible. The phenomena of induced resonance scattering and induced transparency were also studied.

In a parallel second study, we have explored beam waves of the type that are emitted at the output of a prism coupler containing a nonlinear layer along which a surface wave is incident at the input. Because these beam waves can be fully characterized by a leaky wave field, we have extended to nonlinear layers the leaky-wave concept that has so far been restricted to linear configurations. In addition to beam-coupling configurations, this novel field approach to nonlinear media is applicable to a broader class of field varieties.

3. STATE OF THE ART AND PROGRESS DETAILS

Recent work on the interaction of electromagnetic waves with nonlinear dielectric films having intensity-dependent refractive indices has revealed [1,2] a number of remarkable phenomena which have stimulated the development of many ultra-fast and compact all-optical and optoelectronic devices. Besides their compactness, nonlinear thin-film devices have the additional advantage that the waves inside the film can be compressed to a dimension comparable to a wavelength, or even smaller, so that nonlinear processes which depend sensitively on the field intensity can be drastically enhanced [3]. Moreover, the waves can be guided along the film through a great distance, thereby providing a long path for the interaction and mixing of the waves and thus further enhancing the nonlinear effects. However, most theoretical results reported so far in this area have assumed that the incident field is a *plane wave*. This is often an inadequate assumption even in the low intensity (linear) limit. In fact, by considering* incident *bounded beams* instead of plane waves, lateral beam displacements have been identified [4-11] even in linear dielectric or metallic layers. Most recently, we have reported [12] an entire set of fascinating *nonspecular effects* which include not only large lateral beam displacements, but also focal and angular beam shifts, anomalous absorption phenomena and strong beam-profile deformations. Analogous effects occur for transmitted (refracted) beams [9].

In the nonlinear regime, on the other hand, a beam wave can undergo self-focusing or self-fragmentation even in an infinite homogeneous medium [13]. In a one-dimension spatially homogeneous medium, detailed studies have conclusively indicated [14] that the propagation characteristics of nonlinear waves depend crucially on the initial wave profile. Furthermore, a huge lateral beam shift of the Goos-Hänchen type has already been reported [15]. All these considerations indicate that the presence of nonlinear thin films can drastically modify the plane-wave results and significantly magnify nonspecular effects which are large already in the absence of nonlinearities.

Work in this area has also emphasized [2] effects associated with optical-bistability phenomena which, of course, have tremendous potentials for a variety of device applications. However, bistability is associated with an intrinsic nonlinear behavior that has no counterpart in the linear regime and cannot, in fact, exist unless the incident power is above a threshold level [16-18]. By contrast, the phenomena considered here involve nonlinearities which account for fields that are not subject to threshold effects but, in the limit of very weak intensities, their behavior reduces to that of linear media. The nonlinear situations to be studied are therefore inherently different from those leading to bistability and, in particular, they can be regarded as *generalized analogs of the particular linear case*.

The nonlinear generalized analogs addressed by our research program consist of planar configurations that contain one or more layers whose refractivity is field-intensity dependent. A principal concept motivating this research is that, by judiciously combining the effects of nonlinearities with the non-specular behavior of beam fields,

new beam-controlling techniques can be developed for application to thin-film optical components. In this context, our studies during the past period have dealt with the two inter-related aspects outlined below.

A. Propagation of plane waves through media having Kerr-like nonlinearities with negative coefficients.

We have previously carried out [26] an exact analytical study of the scattering of plane TE polarized waves with a nonlinear thin film whose refractivity is a function of the local field intensity. Detailed results were also reported in the case where the film has a Kerr-like optical nonlinearity with a positive (self-focusing) Kerr coefficient. These results have now been extended to the case of a negative Kerr coefficient, and therefore can be applied to a much larger class of nonlinear films. A particularly interesting case is that of a film made up of InSb, which is known to have a remarkably large and negative Kerr coefficient.

An independent work on this problem has recently been published by Chen and Mills [25] whose main results are very similar. However, there are a few but significant differences between their results and ours, which are highlighted below.

Our results apply to any angle of incidence while those in Ref. [25] hold only for normal incidence. We have also shown that, by a suitable choice of scaling of the various parameters, the basic results are generally independent of the incidence angle. In our work, all possible types of behavior within a rather large parameter region of interest were investigated. We have thus found that there are only four universal types of possible behaviors, which depend on the incidence angle and the linear dielectric constants of the film and the adjacent media. The methodology used in Ref. [25] requires that a specific parameter be scanned through a certain range to find particular values which yield a solution consistent with the boundary conditions. This in effect amounts to solving for the roots of a single but very complicated algebraic equation, which can be somewhat non-trivial because multiple roots may occur. In our work, by contrast, we show that a suitable parametrization of the problem can be implemented which avoids the need to solve any equation numerically at all. Our treatment is therefore much simpler. As a result, we were able to study the problem at much greater depth. In particular, the phenomenon of induced resonance scattering can be investigated in detail. The incident intensity at which such resonances occur was calculated as a function of the film thickness. Induced transparency of the film was also studied, and the required intensity has been calculated.

It is important to note that the work in Ref. [25] is restricted to the case in which the Kerr coefficient is positive. On the other hand, their results have been extended to bilayers and superlattices involving nonlinear dielectric layers [27] while our results apply only to a single nonlinear layer.

Our plane wave studies of nonlinear layers are interesting in their own right because of their fundamental importance. Moreover, they form the basis for developing other techniques in the study of bounded beam effects. An important example is the case of leaky waves associated with the coupling of radiation into a nonlinear waveguide structure which is discussed below.

B. Leaky waves guided by nonlinear layers.

In order to study beam-wave (rather than plane-wave) fields in the context of nonlinear media, we have considered the geometry shown in the inset of Fig. 1, which is relevant to prism-coupler problems. For simplicity, we examine TE modes of the monochromatic two-dimensional wave equation for which we seek solutions of the form

$$E(x,z) = F(z) \exp(ik_x x) \exp[i\int \eta(z) dz], \quad (1)$$

where k_x is a complex quantity. For real values of k_x , analytical solutions are available for guided surface waves [19-22] and for homogeneous plane waves [23-26]. However, the field supported by the configuration in Fig. 1 involves leaky waves characterized by complex values of k_x . For such inhomogeneous fields, only numerical solutions in nonlinear regions having infinite extent have been obtained so far [27-30]; furthermore, analytical results are not available and bounded regions such as those required by layers of finite thickness have not been treated. We have therefore developed a semi-analytical procedure for systematically deriving modal (resonant) solutions characterized by complex values $k_x = \beta + i\alpha$. This approach is applicable to both bounded and infinite nonlinear regions.

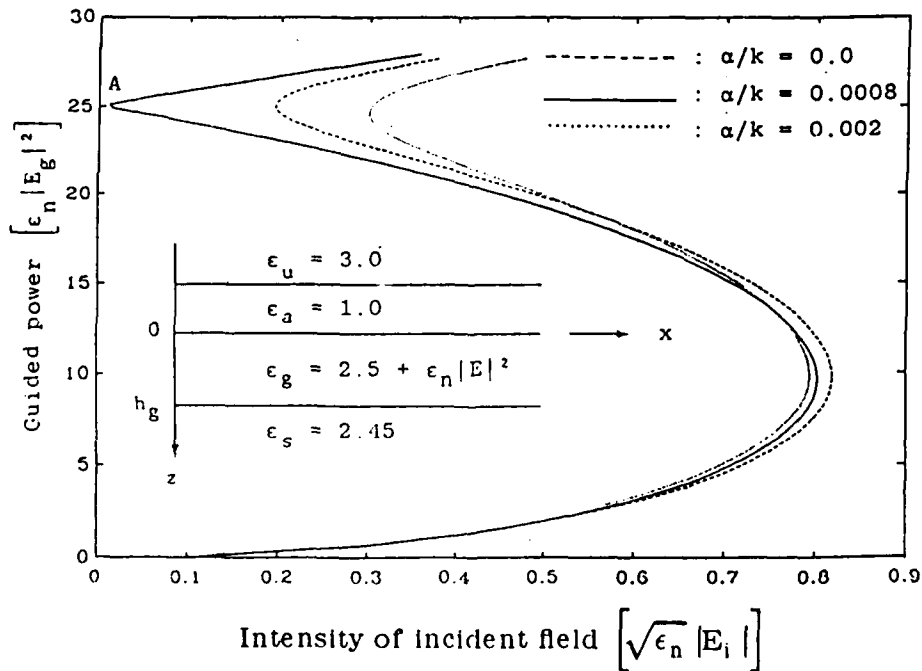


Fig. 1 Variation of power inside the nonlinear layer vs. incident field intensity, for $\beta/k = 1.5715$ and values of α/k .

For that purpose, we introduce Eq. (1) into the pertinent wave equation, suppress the x variable and separate real and imaginary parts to obtain

$$d^2F/dz^2 + [\epsilon(F) - \beta^2 + \alpha^2 - \eta^2(z)]F = 0, \quad (2)$$

$$2\eta(z)(dF/dz) + (d\eta/dz)F - 2\beta\alpha F = 0, \quad (3)$$

which leads to

$$\eta(z)F^2 - 2\beta\alpha \int F^2 dz = \ell, \quad (4)$$

where ℓ is a constant given by the physical parameters involved.

In general, β and α are functions of x if the layered configuration contains a nonlinear region, as is the case for the region with permittivity ϵ_g in Fig. 1. To solve the above equations, a particular cross-section $x = x_0$ is considered where the intensity $F = F_0$ is specified. For that cross-section, an arbitrary complex value of k_x is assumed and we can then find the incident power needed to maintain the specified value of F_0 by using the analytical technique developed by us previously [26].

In this manner, we have generated the curves shown in Fig. 1, which exhibit an interesting instability. More importantly, point A suggests that α and β can be judiciously changed so that no incident power is required to maintain a guided field. Such a situation fulfills the definition of a mode, which in the present case is leaky because $k_x = \beta + i\alpha$ is complex. By next assuming that particular (resonant) value of k_x , the intensity was evaluated at a small distance Δx away from the x_0 cross-section. The values of β, α and $F(x)$ were thus found at all $x > x_0$. The resulting field represents the leaky wave supported by the given nonlinear layer.

We have thus obtained a leaky-wave modal solution having varying values of β and α , as shown in Fig. 2(a). For completeness, Fig. 2(b) shows a comparison between the guided power along x of such a field and that of the conventional leaky wave along a linear layer. Although Figs. 1 and 2 hold for a specific non-linear layer and for a given initial intensity F_0 , the results apply also to other initial $F < F_0$ because smaller values of F simply imply that we start considering the leaky field at transverse planes $x > x_0$. In this sense, Fig. 2 represents universal results which hold for all $F < F_0$ in the given geometry.

In view of the novelty of the above results, we project to continue our study of leaky waves along nonlinear layers. In particular, we shall apply the above method to derive the fields in nonlinear configurations of the prism-coupler variety and other applications.

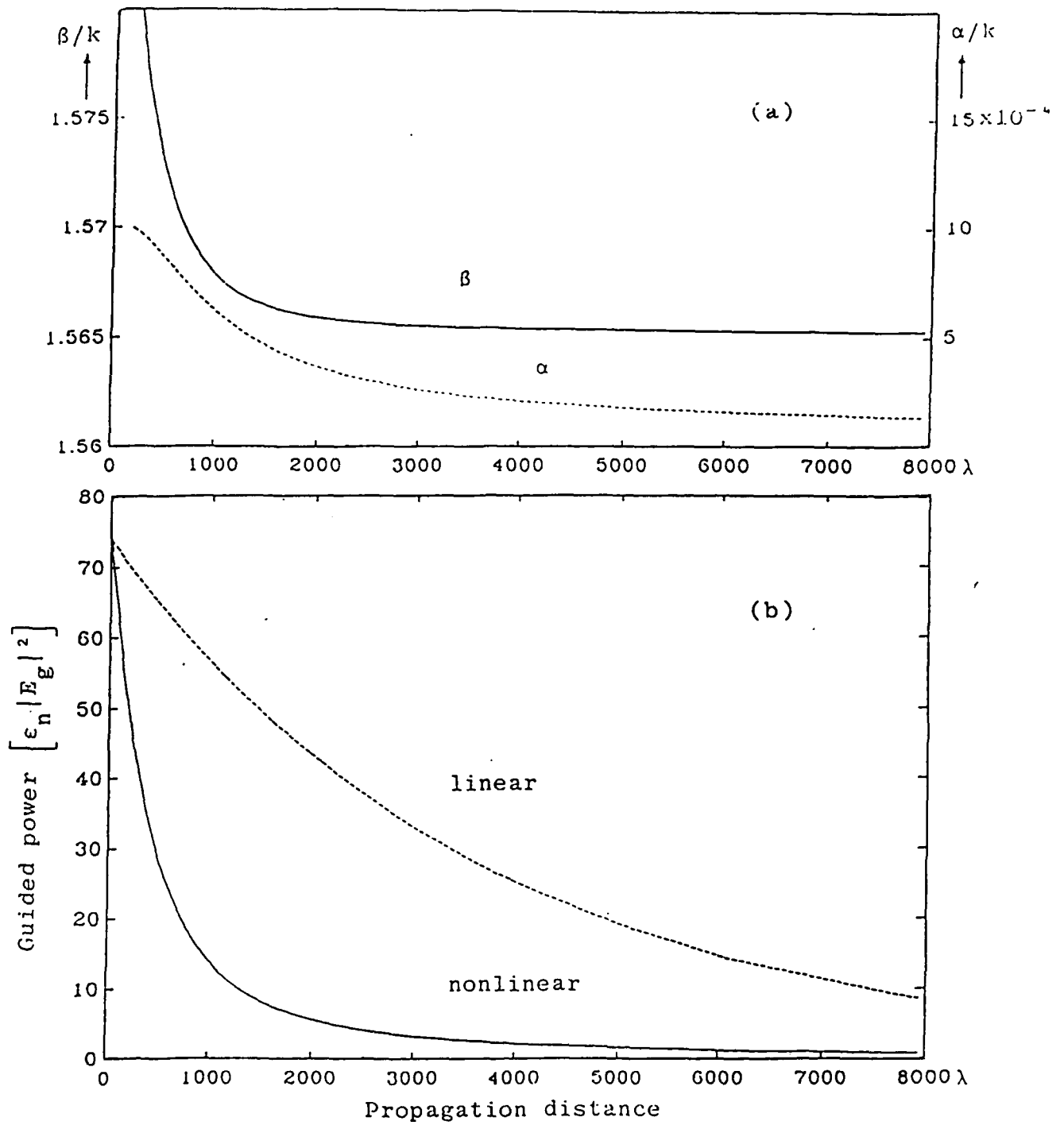


Fig. 2 (a) Variation of β and α vs. distance for the nonlinear layer.
(b) Comparison of guided power vs. distance between linear and nonlinear layers, where $\epsilon_n=0$ in the former.

5. REFERENCES

1. G.I. Stegeman and C.T. Seaton, "Nonlinear surface polaritons", in *Dynamical Phenomena at Surfaces, Interfaces, and Superlattices*, ed. by F. Nizzoli, K. H. Rieder and R.F. Willis (Springer Series in Surface Sciences, Springer-Verlag, NY, 1985).
2. H. M. Gibbs, P. Mandel, N. Peyghambarian, and S.D. Smith, *Optical Bistability III* (Springer-Verlag, NY, 1986).
3. G.I. Stegeman, "Guided wave approach to optical bistability", *IEEE J. Quant. Electron.* QE-18, pp. 1610-1619; October 1982.
4. T. Tamir and H.L. Bertoni, "Lateral displacement of optical beams at multilayered and periodic structures", *J. Opt. Soc. Amer.* 61, pp. 1397-1413; October 1971.
5. W.P. Chen and E. Burstein, "Narrow beam excitation of electromagnetic modes in prism configurations", in *Electromagnetic Surface Modes*, A.D. Boardman, ed. (Wiley, London 1982), pp. 549-574.
6. V. Shah and T. Tamir, "Absorption and lateral shift of beams incident upon lossy multilayered media", *J. Opt. Soc. Amer.* 73, pp. 37-44; January 1983.
7. C.W. Hsue and T. Tamir, "Lateral beam displacements in transmitting layered structures", *Optics Commun.* 49, pp. 383-387; April 1984.
8. P. Mazur and B. Djafari-Rouhani, "Effect of surface polaritons on the lateral displacement of a light beam at a dielectric interface", *Phys. Rev.* B30, pp. 6759-6762; December 1984.
9. C.W. Hsue and T. Tamir, "Lateral displacements and distortion of beams incident upon a transmitting-layer configuration", *J. Opt. Soc. Amer.* A2, pp. 978-988; June 1985.
10. R.P. Riesz and R. Simon, "Reflection of a Gaussian beam from a dielectric slab", *J. Opt. Soc. Am.* A2, pp. 1809-1817; December 1985.
11. S.L. Chuang, "Lateral shift of an optical beam due to leaky surface-plasmon excitations", *J. Opt. Soc. Am.* A3, pp. 593-599; May 1986.
12. T. Tamir, "Non-specular phenomena in beam fields reflected by multilayered media" *J. Opt. Soc. Amer.* A3, pp. 558-565; April 1986.
13. S.A. Akhmanov, A.P. Sukhorukov and R.V. Khokhlov, *Sov. Phys. Uspekhi*, "Self-focusing and diffraction of light in a nonlinear medium", *Sov. Phys. Uspekhi*, 93, pp. 609-636; March-April 1968.
14. M.J. Ablowitz and H. Segur, *Solitons and the Inverse Scattering Transform* (SIAM, Philadelphia, 1981).

15. W.J. Tomlinson, J.P. Gordon, P.W. Smith, and A.E. Kaplan, "Reflection of a Gaussian beam at a nonlinear interface", *Appl. Opt.*, **21**, pp. 2041-2051; June 1982.
16. K.M. Leung, "Propagation of nonlinear surface polaritons", *Phys. Rev. A* **31**, 1189-1192; February 1985.
17. K.M. Leung, "Optical bistability in the scattering and absorption of light from microscopic particles", *Phys. Rev. A* **33**, pp. 2461-2464; April 1986.
18. S. Arnold, K.M. Leung and A.B. Pluchino, "Optical bistability of an aerosol particle", *Opt. Lett.* **11**, pp. 800-802; December 1986.
19. A.D. Boardman, G.S. Cooper, P. Egan, and T. Twardowski, "Properties of nonlinear surface waveguides", pp. 74-78 in Ref. 2.
20. G.I. Stegeman, "Comparison of guided wave approaches to optical bistability", *Appl. Phys. Lett.* **41**, pp. 214-216; August 1982.
20. K.M. Leung, "P-polarized nonlinear surface polaritons in materials with intensity-dependent dielectric functions", *Phys. Rev. B*, **32**, pp. 5093-5101; October 1985.
21. A.D. Boardman and P. Egan, "Optically nonlinear waves in thin films", *IEEE J. Quant. Electron.* **QE-22**, pp. 319-324; February 1986.
22. T. Sakakibara and N. Okamoto, "Nonlinear TE waves in a dielectric slab waveguide with two optically nonlinear layers", *IEEE J. Quant. Electron.* **QE-23**, pp. 2084-2088; December 1987.
23. A.E. Kaplan, "Criterion of existence of longitudinal inhomogeneous traveling waves in nonlinear electrodynamics", *Sov. J. Quant. Electron.* **8**, pp. 95-101; March 1978.
24. A.E. Kaplan, "Theory of plane wave reflection and refraction by the nonlinear interface", in *Optical Bistability*, ed. by C.M. Bowden, M. Cifan, and H.R. Robl, pp. 447-462 (Plenum, NY, 1981).
25. W. Chen and D.L. Mills, "Optical response of a nonlinear dielectric film", *Phys. Rev. B*, **35**, pp. 524-532; January 1987.
26. K.M. Leung, "Scattering of transverse-electric electromagnetic waves with a finite nonlinear film", *J. Opt. Soc. Amer.* **B5**, pp. 571-574; February 1988.
27. W. Chen and D.L. Mills, "Gap solitons and the nonlinear optical response of superlattices", *Phys. Rev. Lett.* **58**, pp. 160-163; January 1988.
28. J. Ariyasu, C.T. Seaton and G.I. Stegeman, "Power-dependent attenuation of nonlinear waves guided by thin films", *Appl. Phys. Lett.* **47**, pp. 355-357; August 1985.

29. P. Arlot and G. Vitrant, "Theoretical study of a nonlinear prism output coupler", Appl. Phys. Lett. **50**, pp. 650-652; March 1987.
30. G.I. Stegeman, G. Assanto, R. Zandoni and C.T. Seaton, "Bistability and switching in nonlinear prism coupling", Appl. Phys. Lett. **52**, pp. 869-871; March 1988.

**SECTION II:
FIELD - PARTICLE INTERACTIONS IN MATTER**

A. RESONANT INTERACTIONS IN CRYSTALS AT X-RAY WAVELENGTHS

Professors G. Schaefer and E.E. Kunhardt

Unit FP8-1

1. OBJECTIVE(S)

The objective of this project is to investigate the possibility of obtaining a non-divergent beam of partially coherent x-ray radiation from the interaction of active oscillators that are either imbedded in or constituting a crystal lattice.

2. SUMMARY OF RECENT PROGRESS

A model has been formulated for investigating the emission properties of one or more identical oscillators imbedded in a host lattice. The "guided-wave" technique of electromagnetic theory¹ has been used to develop the governing equations. Two oscillator(s)-lattice configurations are being investigated for which (a) the excited oscillator(s) are either substitutional or interstitial impurities in the host (non-resonant) lattice, and (b) the host lattice is resonant to the radiation emitted by the oscillators. For the cases of interest, the wavelength of the radiation, λ , is of the order of the oscillator spacing, d . The issues being addressed are: (1) the coupling of the emitted radiation to normal (guided) modes of the lattice, and (2) coherence phenomena in the radiation of the oscillators which can lead to enhanced emission in well-defined directions. This consideration, namely, that the sought emission is into a well-defined direction, more generally, into specific guiding modes of the lattice, makes the guided-wave technique most suitable for the formulation of the radiation problem.

The overall radiation problem has been decomposed into a "modal" problem for determining the guided modal fields of the host lattice (which, as in case (b) above, may resonantly scatter the radiation), and the "emission" problem for the excitation of the guided modes by the active oscillator(s). The symmetry properties of the lattice serve to simplify the modal problem by allowing a decomposition into two: (1) a (microscopic) "field" problem for determining the (resonant for case (b)) scattering from a crystal plane, and (2) a one-dimensional "network" problem of combining this scattering periodically so as to infer the (macroscopic) modal fields of the lattice. The

"field" problem is cast in terms of a single cell scattering leading to a multiple-scattering equation for the scattered wave. In the following section, the basic equations that constitute the theoretical approach outlined above are presented. A classical model has been adopted for the oscillators since it is simple to use and more than adequately serves to illustrate the principles involved.

3. STATE OF THE ART AND PROGRESS DETAILS

The effect on the emission properties of an oscillator due to its interaction with others of the same kind that surround it and are periodically arranged, has been investigated in the limits $\lambda \gg d$ (super-radiant regime)^{2,3} and $\lambda \ll d$.^{4,5} Moreover, this effect has been studied for cases where the interaction is mediated through particles,⁶ photons,^{2,3} and γ and x rays.^{4,5,7} For the last two cases, the investigations have been restricted to the regime $\lambda \ll d$, (by necessity in the case of γ rays). The radiation pattern observed outside a 3-D lattice exhibits a set of light and dark Kossel cones, corresponding to the various internal Bragg reflections. The theory of the Kossel effect for x-rays emitters that are non-resonant with the surrounding oscillators, and its application the determination of the crystal structure, have been extensively discussed in the literature.^{8,9} The corresponding resonant lattice problem for γ rays was treated by Hannon et al.¹⁰

An analogous problem that has received consideration attention recently is that of the effect on the emission properties of an oscillator due to its interaction with a surrounding cavity.¹¹⁻¹³ In this case, the modes of the surrounding medium form a discrete set so that the radiation line width of the isolated oscillator can be significantly altered by the presence of the cavity. In the case of the lattice, even though the modes of the periodically arranged oscillators form a continuum, there are preferred directions for which the radiation line widths may be significantly affected. The degree of the effect depends on the coupling between the oscillators and their coupling to the lattice modes. One interesting possibility is that of mode locking/suppression by increasing the coupling between the oscillator.

Recently, K. Das Gupta published a series of papers¹⁴ reporting results from experiments in which a high intensity source is used to excite various doped crystals. As sources, he has used a focused electron beam and a combination of focused electron beam and characteristic x-radiation of the crystal. Since he has also used a number of configurations and crystals (type and properties), it is not possible to discuss all his observations here. However, the most notable observations are: (a) a

significant narrowing of the fundamental width of the K_α line as the intensity of the sources (pump power) increases, (b) a nonlinear rise with pump power of the intensity of this line, and (c) a beam of negligible divergence.

These results have attracted some attention, both theoretical¹⁵ and experimental¹⁶. However, no satisfactory explanation has been given. Das Gupta qualitatively explains¹⁷ these observations as resulting from an anomalous Kossel emission (arising from the decay of active oscillators inside the crystal).¹⁸ Although it is not clear at this point what really is happening in the crystal, it is reasonable to assume that the behavior of a system comprised of active oscillators and a radiation field may depend on the intensity (and frequency) of the radiation. Thus, as the intensity is increased, nonlinear effects (such as mode coupling, enhanced spontaneous emission into the Borrmann modes, etc.) may be significant and lead to the observation of "anomalous phenomena" reported by Das Gupta.

There exists a wealth of resonant interactions that need to be investigated in this system. Our objective is to maximize the effect by properly choosing the properties of the oscillators (density and radiation wavelengths, for example), and of the host lattice (lattice constant and either resonant or non-resonant scattering). We will focus on the regime for which $\lambda \geq d$. Note that the spacing between the emitting oscillator (or resonant scatterers) need not be the same as the spacing of the host lattice in which the oscillators are imbedded.

As previously mentioned, the analysis of the emission of an oscillator that is surrounded by others (some or all of which may be of the same kind) into well-defined directions is most appropriately formulated using a guided wave representation for the macroscopic fields in the medium. In this report, we discuss that aspect of the problem denoted as the "modal" problem in Section 2. As a model for the overall radiation problem, consider a simple cubic lattice whose sites are at the point $\underline{r}_i = d\underline{s}_i$, where \underline{s}_i is a vector in the direct lattice constant. Suppose that each site is occupied by discrete oscillators which can be represented by a current distribution $\underline{J}_i(\underline{r}_i, t)$, as shown in Fig. 1(a). (Note that in the "emission" problem, we will also consider cases where the active oscillators may be located at points other than the lattice sites, as is the case for example, in interstitially doped crystals.) The lattice may equivalently be viewed as a waveguide whose "walls" maintain the transverse periodicity of the lattice (Fig. 1(b)). A transfer matrix U is defined that relates the modal field state vectors at the longitudinal boundaries B of the unit cell (Fig. 1(c)). Eigenvalues of the transfer matrix U characterize the dispersion relations of the macroscopic modal fields. This calculation constitutes the "network" problem (from

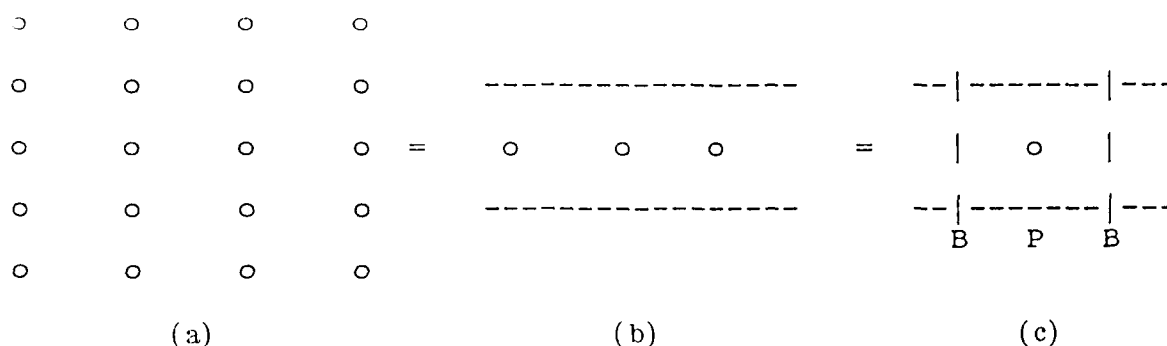


Fig. 1 (a) Periodic arrangement of oscillators (denoted by circle) constituting a crystal. (b) Equivalent "guide" representation. The dashed lines correspond to "guide" walls indicative of transverse periodicity. (c) Equivalent unit cell "field" problem (see text).

Section 2). The explicit calculation of U requires solution at the microscopic level of the resonant scattering of the X-rays by a single element (cell) in the longitudinally infinite guide (Fig. 1(c)), i.e., the "field" problem.

To effect the decomposition of the "modal" problem into a network and field problem, consider a guided coordinate basis where the guiding direction, \underline{a}_z is chosen to be one of the directions of translational symmetry. In this basis,

$$\underline{1} = \underline{a}_z \underline{a}_z + \underline{a}_t \underline{a}_t = \underline{1}_L + \underline{1}_t \quad (1)$$

where \underline{a}_t is a vector transverse to \underline{a}_z . Introduce a basis of orthogonal functions (modes)

$$\underline{\phi}(\underline{\rho}) = \frac{e^{i(\underline{k}_t + \underline{h}_i) \cdot \underline{\rho}}}{\sqrt{\sigma}} \underline{a}_p \quad (2)$$

where $\underline{\rho}$ is the radius vector transverse to \underline{a}_z , \underline{k}_t is a (two-dimensional) prescribed, but arbitrary transverse wavenumber, \underline{h}_i is a (two-dimensional) reciprocal transverse lattice vector, \underline{a}_p is a (two-dimensional) polarization vector, and σ is the area of the transverse unit cell. The mode functions, Eq. (1), possess the orthogonality properties

$$\iint \underline{\phi}_i^*(\underline{\rho}) \cdot \underline{\phi}_j(\underline{\rho}) ds = \delta_{ij} \quad (3)$$

in the transverse plane of a unit cell. These mode functions can be used to represent the radiation field with prescribed \underline{k}_t everywhere in the lattice.

$$\underline{E}(\underline{r}) = \sum_i a_i(z) \underline{\phi}_i(\underline{\rho}) = \sum_i \underline{E}_i(\underline{r}) \quad (5)$$

In a $e^{-i\omega t}$ basis, Maxwell's equations may be written in the form

$$\left[\nabla_x \nabla_x \underline{\underline{1}} - \mu_0 \epsilon_0 \omega^2 \underline{\underline{1}} \right] \underline{E} = i\omega \mu_0 \underline{J} \quad (4a)$$

Letting $\underline{J} = L_0^{-1} \underline{E}$, where L_0^{-1} is the inverse of the oscillator operator, Eq. (4a) becomes

$$\left[\nabla_x \nabla_x \underline{\underline{1}} - L_p^{-1} - k_0^2 \underline{\underline{1}} \right] \underline{E} = 0 \quad (4b)$$

where

$$k_0^2 = \omega^2 \mu_0 \epsilon_0 \quad (4c)$$

For the time independent electric field

$$\underline{E}(\underline{r}) = \sum_i a_i(z) \underline{\phi}_i(\underline{\rho}) = \sum_i \underline{E}_i(\underline{r}) \quad (5)$$

Using Eq. (5) in (4), we obtain for the modal amplitudes in the interstitial regions (where the currents are assumed to be zero)

$$\left[\frac{d^2}{dz^2} + \kappa_i^2 \right] a_i(z) = 0 \quad (6a)$$

where

$$\kappa_i = \sqrt{k_0^2 - (\underline{k}_t + \underline{h}_i)^2} \quad (6b)$$

In regions where the currents are not zero, the representation (4) still holds but the coefficient equations (6a) are coupled. Thus in the interval where Eq. (6a) holds, it is evident that the field is representable via (4) as a superposition of plane wave modes of the form

$$\underline{\Phi}_{\pm i} = e^{\pm i\kappa_i z} \phi_i(\rho) \quad (7)$$

which are propagating or attenuating along z , depending respectively on whether $\kappa_i^2 > 0$ or $\kappa_i^2 < 0$. In the case of a rectangular transverse lattice with unit cell of sides a and b ,

$$\underline{h}_i = \frac{2\pi m}{a} \underline{a}_x + \frac{2\pi n}{b} \underline{a}_y, \quad m, n = 0, \pm 1, \pm 2, \dots$$

From Eq. (6b), for sufficiently low k_0 , of the order of $(\pi/a, \pi/b)$, only two modes, $i=0$ and $i=1$ are propagating. The evanescent behavior of the higher $i > 1$ modes implies that the representation (4) is rapidly convergent at a point between the atomic planes. In consequence, the dominant mode component of $E(\underline{r})$, viz:

$$\underline{E}_0(\underline{r}) = (a_0^+ e^{i\kappa_0 z} + a_0^- e^{-i\kappa_0 z}) \phi_0(\rho) \quad (8a)$$

$$\underline{E}_1(\underline{r}) = (a_1^+ e^{i\kappa_1 z} + a_1^- e^{-i\kappa_1 z}) \phi_1(\rho) \quad (8b)$$

provide a good first approximation to $E(\underline{r})$ at such points. Although higher mode contributions can be readily included, the subsequent analysis will, for the most part, characterize the "macroscopic" behavior of $E(\underline{r})$, i.e., the behavior at the midplanes in terms of the dominant modal description in Eqs. (8). In Eqs. (8), the quantities a^\pm represent the amplitude of waves travelling toward and away from an atomic plane at $z=0$. They assume different values on opposite sides of the plane. The knowledge of the discontinuities in the values of a^+ and a^- , which are induced by the resonant scattering at the atomic plane, permits a ready calculation of the macroscopic behavior of the field. Thus, the field problem is cast into that of ascertaining the discontinuities in a^\pm from the resonant scattering properties of an atomic plane. By linearity considerations, preliminary to explicit solution of the scattering problem, one can ascertain the nature of the relation between the a^+ and a^- . This in turn permits one to infer the plane to plane variation of the guided wave amplitudes a^+ and as well the dispersion relation for such waves, i.e., the network problem.

Linearity implies, in matrix notation, that

$$\begin{bmatrix} a_R^+ \\ a_R^- \end{bmatrix} = \begin{bmatrix} u_{11} & u_{12} \\ u_{21} & u_{22} \end{bmatrix} \begin{bmatrix} a_L^+ \\ a_L^- \end{bmatrix} \quad (9)$$

where the subscripts R and L refer respectively to the right or left of the atomic planes, and (u_{ij}) denotes a "transfer" matrix characterizing the discontinuities in a^\pm induced by the scattering atom. If one introduces the wave vector notation characterizing the dominant guided wave amplitudes at the n^{th} mid-plane

$$\underline{\xi}_n = \begin{bmatrix} a_o^+ [(n - 1/2)d] \\ a_o^- [(n - 1/2)d] \\ a_1^+ [(n - 1/2)d] \\ a_1^- [(n - 1/2)d] \end{bmatrix}$$

We can rewrite Eq. (9) for the guided wave amplitudes at $z = d/z$ and $z = -d/z$ as

$$\underline{\xi}_1 = U \underline{\xi}_o \quad (10)$$

where

$$U = \Theta(u_{ij})\Theta$$

where (u_{ij}) is now a 4x4 matrix and

$$\theta = \begin{bmatrix} e^{i\theta_o/2} & 0 & 0 & 0 \\ 0 & e^{-i\theta_o/2} & 0 & 0 \\ 0 & 0 & e^{i\theta_1/2} & 0 \\ 0 & 0 & 0 & e^{-i\theta_1/2} \end{bmatrix}$$

with $\theta_i = \kappa_i d$. The translational invariance of the lattice requires that

$$\hat{a}^\pm [(n + 1/2)d] = \lambda \hat{a}^\pm [(n - 1/2)d] \quad (11)$$

where the $\hat{}$ distinguishes the guided wave amplitudes that compose a translationally invariant mode, i.e., a Bloch wave, and λ is a translation factor independent of n . From Eqs. (11) and (10), one obtains

$$U \hat{\xi}_i = \lambda_i \hat{\xi}_i \quad (12)$$

that determines both the translation factors λ_i and the relation between the guide wave amplitudes \hat{a}_\pm for the modal Bloch wave.

The explicit evaluation of Eq. (12) requires the solution of the problem of scattering of a plane wave Φ_i of Eq. (7) by a single atomic plane (Fig. 1c). This plane is characterized by source currents with two-dimensional periodicity which are assumed to be localized near the center of a cell. For this purpose we introduce a free space Green's function, $\underline{\underline{G}}(\underline{r}, \underline{r}')$ which has the transverse periodicity of the lattice and is defined within a unit cell by

$$[\nabla_x \nabla_x \underline{\underline{1}} - k_0^2 \underline{\underline{1}}] \underline{\underline{G}}(\underline{r}, \underline{r}') = -\delta(\underline{r} - \underline{r}') \underline{\underline{1}} \quad (13)$$

subject to the requirements,

$$\begin{aligned} \underline{\underline{G}}(\underline{r}, \underline{r}') &\rightarrow 0 \text{ as } |\underline{r} - \underline{r}'| \rightarrow \infty \text{ if } \text{Im } \kappa_0 > 0 \\ \underline{\underline{G}}(\underline{r} + \underline{\rho}_i, \underline{r}') &= \underline{\underline{G}}(\underline{r}, \underline{r}') e^{i\kappa_0 \cdot \underline{\rho}_i} \end{aligned}$$

where $\underline{\rho}_i$ is a transverse lattice vector and k_0^2 is given by Eq. (5c). In a basis noted in Eqs. (2) and (7), the solution to Eq. (13) is discontinuously represented by

$$\underline{\underline{G}}(\underline{r}, \underline{r}') = \begin{cases} \sum_j \frac{1}{2i\kappa_j} \underline{\Phi}_j(\underline{r}) \underline{\Phi}_{-j}(\underline{r}') & z > z' \\ \sum_j \frac{1}{2i\kappa_j} \underline{\Phi}_j(\underline{r}') \underline{\Phi}_{-j}(\underline{r}) & z < z' \end{cases} \quad \begin{matrix} (14a) \\ (14b) \end{matrix}$$

The Green's function $\underline{\underline{G}}(\underline{r}, \underline{r}')$ provides the means for transforming the relevant wave equation for \underline{E} into the integral equation,

$$\underline{E}_i(\underline{r}) = \underline{\Phi}_i(\underline{r}) - \int \underline{\underline{G}}(\underline{r}, \underline{r}') L_0^{-1} \underline{\Phi}_i(\underline{r}') d\underline{r}' \quad (15)$$

where the volume integral $d\underline{r}'$ is extended only over one sphere of radius R about the

scattering atom. To the right and left of the atomic plane at $z=0$, one infers from Eqs. (14) that

$$E_i = \Phi_i(\underline{r}) + \sum_j \frac{1}{2i\kappa_j} \Phi_j(\underline{r}) T_{ji} \quad z > R \quad (16a)$$

$$\Phi_i(\underline{r}) + \sum_j \frac{1}{2i\kappa_j} \Phi_j(\underline{r}) T_{ji} \quad z < -R \quad (16b)$$

where R denotes the distance from the atomic plane beyond which the current distribution is zero, and where

$$T_{ji} = \int \Phi_{-j}(\underline{r}) \cdot L_p^{-1} E_i(\underline{r}) d\underline{r} \quad (17)$$

denotes the j^{th} element of a transition matrix T indicative of the degree of excitation of the j^{th} guided mode Φ_j by an incident mode Φ_i .

The above formulation of the scattering problem in terms of a guided wave basis Φ_i , characteristic of the transverse periodicity of the lattice, provides a simple expression, Eq. (17), for the elements of the transition matrix.] Knowing T_{ji} , the elements of the transfer matrix U , Eq. (10), can be evaluated. The explicit evaluation of these components is more conveniently carried out in an alternative (spherical) guided wave basis

$$\phi_\mu(\underline{r}) = j_m(\kappa_0 r) Y_{mn}(\theta, \phi) \quad (18)$$

where j_m is the spherical Bessel function and Y_{mn} are the spherical harmonics. The details of these calculations will be presented in a subsequent report, together with the solution to the "emission" problem (see Section 2).

4. REFERENCES

1. N. Marcuvitz, *Waveguide Handbook*, (McGraw Hill, New York) Chapters 1-3.
2. R. H. Dicke, *Phys. Rev.* **93**, 99 (1954).
3. V. M. Fain, *Usp. Fiz. Nauk* **64**, 273 (1958).
4. M. I. Podgoretskii and I. I. Roizen, *Soviet Phys.-JETP* **12**, 1023 (1961).

5. C. Muzikar, Soviet Phys.-JETP 14, 833 (1962).
6. A. M. Afanas'ev and Y. Kagan, Soviet Phys.-JETP 21, 215 (1965).
7. J. P. Hannon and G. T. Trammell, Phys. Rev. 169, 315 (1968).
8. R. W. James, *The Optical Principles of the Diffraction of X-rays*, (Cornell Univ. Press, Ithaca, NY, 1965) pp. 413-457.
9. R. Tixier, C. Wache, J. Appl. Crystallog. 3, 466 (1970).
10. J. P. Hannon, N. J. Carron, and G. T. Trammell, Phys. Rev. B 9, 2791 (1974).
11. P. Stehle, Phys. Rev. A 2, 102 (1970).
12. D. Kleppner, Phys. Rev. Lett. 47, 233 (1981).
13. G. Gabrielse and H. Dehmelt, Phys. Rev. Lett. 55, 67 (1985).
14. K. Das Gupta, Physics Letters, 46A, 197 (1973); Phys. Rev. Letters, 33, 1415 (1974); Physics of Quantum Electronics, 5, 381 (1978).
15. S. A. Akhmanov and B. A. Grishanin, JETP Letter, 10, 517 (1976).
16. P. Eisenberger, N. G. Alexandropoulos and P. M. Platzman, Phys. Rev. Letters, 28, 1519 (1972).
17. K. Das Gupta, private communication.
18. B. W. Batterman and H. Cole, Rev. Mod. Phys. 36, 681 (1964).

B. RESONANCES IN X-RAY PHONON INTERACTIONS IN CRYSTALS

Professor H.J. Juretschke

Unit FP8-2

1. OBJECTIVE(S)

The development of a dynamical theory of x-ray phonon interactions that is adequate for proper treatment of these interactions under conditions where the conventional description leads to singularities. It is expected that these singularities are indicative of resonances. Therefore, a second objective is the study of the role of these resonances in enhancing the coupling to a level of practical experimentation on the interaction of x-rays with IR-laser induced polaritons. A third objective is the optimization of the nonresonant background coupling of such interaction by proper choice of the host crystal, and the IR frequency, as well as the x-ray diffraction planes.

2. SUMMARY OF RECENT PROGRESS

The work on this program has progressed in a number of directions. Some of these concern consequences or completion of earlier results, others deal with the initial work on the new phase that followed from the recent proposal as given above.

In brief, two new papers deal with special applications of the approximate theory of x-ray propagation near n-beam points, showing, in one case, that the influence of n-beam points is pervasive, and cannot be ignored in high precision work, and in the second, that the interpretation of asymmetries in intensities in this region may have more than one origin. An experimental program on verifying some of the further consequences of this theory was carried out at Brookhaven this summer, and, while the copious results remain to be studied in detail, they seem to have revealed features which have not been observed so far. The new program has been initiated by developing a degenerate perturbation theory applicable to the x-ray problem, and by testing it out on the earlier theories of x-ray coupling; and also by organizing a computer program for a systematic survey of likely strong x-ray polariton configurations.

3. STATE OF THE ART AND PROGRESS DETAILS

The areas mentioned in Section 2 above are reviewed here in more detail.

1) A study of the influences of n-beam interactions on the precision determination of 2-beam structure factors has been published [1]. This work called attention to the almost universal need of n-beam corrections whenever one wants to determine structure factors to an accuracy better than one part in 10^4 . Long-range influences of this order of magnitude exist everywhere in diffraction space, and must be taken into account when interpreting the data, especially when these are to be compared with theoretical models or predictions. In order for such correction to be successful, however, it is essential that experimental results are accompanied by specifying their complete embedding in reciprocal space. This is needed to identify the pertinent leading correction terms, which can then be applied from previous, standard accuracy, knowledge of the parameters of these n-beam interaction points.

2) A detailed theoretical analysis of some new experimental data on the special case of the interaction of a strong primary beam with weak secondary beams has shown that the theoretical formulation published earlier [2] is in quantitative agreement with the experimental results. This is the first case in which the effect of the modification of absorption in the neighborhood of an n-beam interaction leads to important corrections of the usual interpretation of the asymmetry of the integrated intensity in the neighborhood of the n-beam point. A paper on this work has been accepted for publication in *Acta. Cryst. A* [3].

3) This past summer, in collaboration with N. Alexandropoulos (Visiting Research Professor at the Polytechnic, permanent position at the University of Ioannina, Greece), an experimental test was undertaken in order to investigate the recent prediction [4] of the differences in the intensity asymmetries near an n-beam point shown by x-rays of differing polarization. This work was carried out on a beam line at the Brookhaven synchrotron, with the diffractometer positioned in such a way that the silicon crystal saw either σ - or π -polarized incident radiation. In fact, the resolution of the π -beam was such that it was impossible to obtain integrated intensities experimentally by direct measurement. These have to be evaluated by integration over the rocking curve, determined with a second of arc resolution. As a consequence, we also obtained detailed results for rocking curves in the neighborhood of the n-beam point; they showed occasional anomalies that had been anticipated (4), but whose full physical interpretation remains to be understood. The more than 800 experimental scans obtained in the period of a few weeks will begin to be analyzed systematically in the near future.

4) Work has begun on extending the second order perturbation theory for describing x-rays near an n-beam point developed earlier [6] into the most interesting region where this problem becomes degenerate, so that the solutions obtained so far diverge. This will be used as a trial problem in which to explore the usefulness of the

techniques that are to be applied also to the problem of resonances (degeneracies) in the x-ray-phonon interaction, the major topic of the current proposal. It has already been shown by the results so far that, other than in a few exceptional cases, the general methods of degenerate perturbation theory can also be formulated such as to be applicable to the interactions of interest here. In their own right, the results have led to a new formulation of the problem originally discussed a few years ago [7]; this formulation can be characterized as the optimal effective two-beam representation of the n-beam problem. The implications of this approach, especially relative to various outstanding issues concerning practical applications of the n-beam region, are being explored intensively at present.

5) A general computer program is being developed for allowing a systematic survey of the nonlinear x-ray-polariton response in various polar materials, over a range of wavelengths, and for selected diffraction conditions. This survey is one of the fundamental needs in developing a proposal for a concrete experiment demonstrating the dynamical interaction of lasers with x-rays.

4. REFERENCES

1. H. J. Juretschke and H. K. Wagenfeld " A Simple Method for Estimating the Contribution of Neighbouring N-beam Interactions to Two-beam Structure Factors," Australian J. Phys., **41**, 469 (1988).
2. H. J. Juretschke, "First Order Asymmetry in the Renninger Interaction of a Strong Primary Reflection with Weak Beams," Acta. Cryst., **A42**, 405 (1986).
3. H. J. Juretschke, "Comments on 'The Phases of Forbidden Reflections', by B. Post and J. Ladell (1987)," Acta. Cryst. **A**, to be published.
4. H.J. Juretschke, "Anomalous Asymmetries in X-ray π -modes Near N-beam Interactions," Phys. Stat. Sol., (b) **135**, 455 (1986).
5. H.J. Juretschke, unpublished.
6. H. J. Juretschke, "Modified Two-beam Description of X-ray Fields and Intensities near a Three-beam Diffraction Point. Second-order Solution," Acta. Cryst., **A42**, 449 (1986).
7. H. J. Juretschke, "Modified Two-beam Description of X-ray Fields and Intensities near a Three-beam Diffraction Points. General Formulation and First Order Solution," Acta. Cryst. **A40**, 379 (1984).

C. NON-EQUILIBRIUM EM WAVE-COOPER PAIR INTERACTION IN HIGH T_C SUPERCONDUCTORS

Professors E. Wolf, P. Riseborough and E. Kunhardt

Unit FP8-3

1. OBJECTIVE(S)

This work seeks to determine the characteristic times for relaxation processes in cuprate superconductors. Comparison of such times and the relevant temperature dependence with theory is likely to constrain the possible mechanisms for pairing in these materials, and provide a different means of determining certain parameters of the superconducting state. For example, the temperature dependence of the quasiparticle recombination time provides a means of determining the energy gap parameter, for which the most obvious methods, infrared optical absorption and electron tunneling, have provided conflicting results.

2. SUMMARY OF RECENT PROGRESS

Progress has been made toward fabricating thin film samples of the $R\text{Ba}_2\text{Cu}_3\text{O}_{7-x}$ compounds, where R is Dy and Sm, by thermal coevaporation of R, BaF_2 , and Cu. Three rate controllers and an additional quartz microbalance have been installed in a diffusion pumped evaporator with base pressure of 10^{-7} Torr. The additional thickness monitor, mounted on the lower surface of a shutter, is found necessary to normalize the rates of deposition on the substrate from the three separate sources. Oxygen is introduced in the region of the MgO or SrTiO_3 substrates, at a local pressure in the 0.1 to 1.0 Torr range with the chamber pressure in the 10^{-5} range. Rutherford Backscattering (RBS) measurement of the composition of a typical film after oxygen anneal at 850°C showed deficiency of Cu and also showed a decrease in oxygen concentration from the outer surface of the film toward the substrate interface. The reason for weak Cu incorporation is not known with certainty, but may arise in part from the tendency of Cu evaporated films, used to calibrate the thickness monitors, to condense at less than bulk density. We have also made Auger Spectroscopy measurements on the films, in rough agreement with the RBS results.

A commercial helium refrigerator, capable of reaching 10°K with optical windows and fast electrical and microwave coaxial line access has been purchased [1].

3. STATE OF THE ART AND PROGRESS DETAILS

Optically generated quasiparticles can be detected by use of a biased quasiparticle tunnel junction. However, little progress has been achieved toward fabricating

reliable quasiparticle junctions on the cuprate superconductors. Effort has been directed toward the alternative use of Sharvin type metal microcontacts of gold or silver to determine the energy gap of the material [2]. In this case, a nominal 100 Angstrom layer of the metal is evaporated onto the cuprate superconductor, and a mild heat treatment in oxygen performed. This proposal is based on the success of annealed gold and silver deposits in making excellent Ohmic contacts to the cuprate superconductors [3] and the conceptual singularity to Proximity Tunneling Spectroscopy methods which are also based on Andreev scattering [4]. A small cryogenic scanning tunneling microscope is being used to test the properties of such microcontacts.

On the theoretical side, the nonequilibrium properties of the high T_c superconducting materials pose a difficult challenge. The difficulty stems from the dense nature and the strong interactions between the quasi-particles, thereby invalidating the assumptions necessary for the usual Boltzmann equation approach to apply [5]. This problem is exacerbated by the very nature of the underlying electronic states being poorly defined, in that the effects of the Coulomb correlations are strong and cannot be included by standard manybody techniques. Therefore, it has been decided to find an expansion parameter other than the strength of the Coulomb interaction. One alternative parameter is N , the degeneracy of the d orbitals of the Cu atom. A boson version of this expansion has been previously formulated [6-9]. We have shown that the effects of the Coulomb interaction may be organized in powers of $1/N$. To lowest order in $1/N$, we obtain a soluble two band mean field theory which retains the full periodic translational invariance of the underlying lattice. The non-trivial effects of the Coulomb correlations and fluctuations first occur to order $1/N$.

This level of approximation is also tractable. We have shown that this approximation satisfies Luttinger's theorem [10] and is also periodic translationally invariant. We have calculated the electronic Green's function to order $1/N$ which yields both the one electron density of states and the associated lifetimes of these states. Knowledge of these quantities is sufficient to calculate rates for non-equilibrium processes from the standard Boltzmann approach. However preliminary calculations show that such an approach would lead to spurious results. In fact, using Ward identities we have shown that transport processes when calculated correctly to order of less than $1/N^2$ must vanish identically. This cancellation is a specific case of a general result due to Peierls [11] concerning steady state flows. We intend to calculate the $1/N^2$ contribution to the self energy which on utilizing Ward identities [12,13] will directly provide us with the frequency dependent conductivity, or the optical response of these systems. In order to obtain finite results, it is necessary to include the Umklapp processes due to the underlying lattice structure.

The calculation of the order $1/N^2$ terms is also necessary in order to estimate the possible convergence or asymptotic nature of the expansion.

REFERENCES

1. Model LTS-22, available from RMC Cryosystems, Tucson, Arizona
2. P. C. van Son, H. van Kempen, and P. Wyder, Phys. Rev. Lett. **59**, 2226 (1987).
3. Y. Tzeng, A. Holt, and R. Ely, Appl. Phys. Lett. **52**, 155 (1988).
4. J. Ziman, "Electrons and Phonons," Cambridge University Press
5. E. Wolf and G.B. Arnold, Physics Reports **91**, 31 (1982).
6. P.S. Riseborough, Solid State Commun. **8**, 901 (1983)
7. P.S. Riseborough, Z. Phys B. **57**, 289 (1984)
8. P.S. Riseborough and P. Kumar, J.Phys. Lett C **21** 185 (1988)
9. P.S. Riseborough and P. Kumar, J.Phys. C to be published
10. J.M. Luttinger, Phys. Rev. **119** , 1153, (1960) J.M.Luttinger, Phys Rev **121** , 942, (1961)
11. R.Peierls, "Quantum theory of Solids," Oxford University Press
12. P.S. Riseborough, Phys Rev **B27** , 5775 (1983)
13. H.Chang and P.S. Riseborough to be published